- Multiproxy study assessing Holocene environmental change in the Limfjord, Denmark.
- Three large salinity shifts occurred in at Kilen (Limfjord) between 7,500-1,500 BP.
- Kilen was regularly stratified with high marine productivity before 4,400 BP.
- Near fully marine salinity after 4,400 BP and abrupt shift to brackish water at 2,000 BP.
- Changes in salinity/productivity driven by regional climate and hydrographic factors.

Environmental change in the Limfjord, Denmark (ca.7,500-1,500 cal. yrs BP): a multiproxy study

Jonathan P. Lewis[a,b], David B. Ryves[a], Peter Rasmussen[c], Karen L. Knudsen[d], Kaj S. Petersen(†)[c], Jesper Olsen[e,f], Melanie J. Leng[b,g,h], Peter Kristensen[d], Suzanne McGowan[h], and Bente Philippsen[e]

[a] Centre for Hydrological and Ecosystem Science, Department of Geography, Loughborough University, Loughborough LE11 3TU, UK.

Email: (DBR) d.b.ryves@lboro.ac.uk

[b] NERC Isotope Geoscience Laboratory (NIGL), British Geological Survey, Keyworth Site, Nottingham, NG12 5GG, UK.

Email (JL) jwis@bgs.ac.uk; (MJL) mjl@bgs.ac.uk

[c] Department of Marine Geology and Glaciology, Geological Survey of Denmark and Greenland (GEUS), Øster Voldgade 10, DK-1350 Copenhagen K, Denmark.

Email: (PR) per@geus.dk

[d] Department of Geoscience, Aarhus University, Høegh-Guldbergs Gade 2, DK-8000 Aarhus C, Denmark.

Email: (KLK) karenluise.Knudsen@geo.au.dk; (PK) peterk@post10.tele.dk

[e] Department of Physics and Astronomy, Aarhus University, Høegh-Guldbergs Gade 2, DK-8000 Aarhus C, Denmark.

Email: (JO) jesper.olsen@phys.au.dk; (BP) bphilipp@phys.au.dk

[f] School of Geography, Archaeology and Palaeoecology (GAP), Queen's University, Belfast BT7 1NN, Northern Ireland, UK.

[g]Department of Geology, University of Leicester, Leicester, LE1 7RH, UK.

[h] School of Geography, University of Nottingham, Nottingham NG7 2RD, UK.

Email: (SM) suzanne.mcgowan@nottingham.ac.uk

Corresponding author: Jonathan P. Lewis (jwis@bgs.ac.uk). Tel. +44 (0)115 936 3608

Abstract

The Limfjord region of northern Jutland, Denmark, supports a rich archaeological record dating back to the Mesolithic, which documents long-term change in human practices and utilisation of marine resources since approximately 7,500 BP. The presence and availability of marine resources in the Limfjord is sensitively regulated by environmental parameters such as salinity, sedimentary regime, nutrient status and primary productivity, but long-term changes in these parameters are currently poorly understood. In this study a multiproxy approach (including sedimentary parameters, diatoms, molluscs, foraminifera, sedimentary pigments, C and O stable isotopes and plant macrofossils) has been adopted to assess environmental change over the period ca. 7,500-1,500 cal. yrs BP at Kilen, a coastal fjord (before AD 1856) situated in the Western Limfjord. A diatom-based salinity transfer function based on a pan-Baltic training set has been applied to the fossil diatom dataset for quantitative assessment of salinity change over the study period. This study demonstrates that large-scale shifts in salinity are a common feature of the Limfjord's long-term history and are driven by the level of connection with the North Sea and the Skagerrak respectively, which in turn is likely driven by the complex interplay between climate, sea-level change, current velocity and rates of erosion/sedimentary accretion. Three shifts in state at Kilen are identified over the study period: a deep, periodically stratified fjord with medium-high salinity (and high productivity) between ca. 7,500-5,000 BP , followed by a gradual transition to a shallow benthic system with more oceanic conditions (i.e. higher salinity, lower productivity, slower sedimentary accumulation rate and poorer fossil preservation) after ca. 5,000 BP and no stratification after ca. 4,400 BP, and lastly, within this shallow phase, an abrupt shift to brackish conditions around 2,000 BP. Environmental-societal interactions are discussed on the basis of the data presented in this study and current environmental hypotheses for cultural change are challenged.

Key Words

Limfjord, Kilen, salinity, diatoms, sedimentary pigments, molluscs, foraminifera, Holocene, productivity, coastal

1. Introduction

The economic and societal importance of the inner Danish coastal waters (including estuaries and fjords) over many millennia is well documented (e.g. Rasmussen, 1968; Enghoff, 1999; Andersen, 2007; Poulsen et al., 2007; Enghoff, 2011), with these habitats commonly offering a wide range of resources, easily accessible from relatively shallow waters. The Limfjord is a sound situated in the northern part of Jutland, Denmark, connected to the Kattegat in the east and the North Sea in the west (Figure 1a). Today, the Limfjord hosts a large shellfish industry, particularly *Mytilus edulis* (blue mussel) and *Ostrea edulis* (European flat oyster), but in the past has provided important fishing and breeding grounds for several finfish species, including eel, plaice, herring and whitefish (e.g. Enghoff, 1999; Poulsen et al., 2007). Furthermore, the presence of Stone Age shell middens and other archaeological sites (Figure 1b), dominated by marine molluscs (particularly oysters in the late Mesolithic, prior to their

widespread decline at the Mesolithic-Neolithic transition; Andersen, 2007), but also containing fish bones (from marine, brackish and freshwater species) along its former coastlines suggests a long history of habitation and exploitation (e.g. Madsen et al., 1900; Andersen and Johansen, 1986; Andersen, 1995a; Enghoff et al., 2007).

Despite its cultural importance, the long-term natural environmental history of the Limfjord is poorly understood. The few studies that exist for this region focus predominately on the last 2,500 years, when sea level was close to its present level (e.g. Gehrels et al., 2006) and subsequently the Limfjord was a particularly dynamic environment, subject to fluctuating salinities associated with the degree of exposure to the North Sea and Skagerrak (Kristensen et al., 1995; Christensen et al., 2004; Ryves et al., 2004; Lewis, 2011; Mertens et al., 2011). However, studies extending back further than 2,500 yrs BP are poorly dated, have low temporal resolution and lack any attempt to quantify changes in salinity (e.g. Petersen, 1981; Andersen, 1992a; Heier-Nielsen, 1992).

This paper presents results from a high-resolution, multiproxy study, analysing changes in the marine environment at Kilen, a small semi-isolated basin of the Western Limfjord, between ca. 7,500-1,500 cal. yrs BP (hereafter "BP"),. Changes in salinity, productivity, hydrography and sedimentation at this site are inferred from sedimentary parameters, diatoms, foraminifera, molluscs, plant macrofossils and sedimentary pigments. A diatom-based transfer function is employed to produce quantitative salinity estimates over the study period derived from a large, existing pan-Baltic training set (Andrén et al., 2007). Environmental hypotheses for cultural change are reviewed on the basis of the new evidence presented here, including the long-debated possible environmental events at the Mesolithic-Neolithic transition (Rowley-Conwy, 1984) as seen from the perspective of the western Limfjord.

This study is particularly important as it the first long-term, multiproxy record, with good chronological control from the Limfjord region covering all three major phases of shell midden accumulation (ca. 7,400-5,200 BP, 4,800-4,400 BP and 2,500-1500 BP; Andersen, 2007). Furthermore, long-term data on natural environmental variability are urgently needed in the context of growing awareness of, and concern with, coastal and marine environmental change throughout the Baltic Sea region (Conley et al., 2009; Kabel et al., 2012; Neumann et al., 2012 and references therein).

2. Study area

Kilen (56º30.005"N, 08º34.089"E) is a shallow eutrophic 'lake' situated in the western Limfjord (northern Jutland) in the Danish commune of Struer (Figure 1). It is classified as a brackish-water lake (~6 g L^{-1} total dissolved solids), following its almost complete separation from the Limfjord by the building of a road and rail embankment in AD 1856. A connection with the Limfjord is retained via a small stream in the south-east corner (Figure 1c) and is important for maintaining brackish salinity levels. The 'lake' is approximately 5 km long, 1 km wide with a total area of 3.34 km^2, an average water depth of 2.9 m and a maximum depth of 6.5 m (Windolf et al., 1996; Jensen et al., 2006).

3. Methodology

In April 2007, a 15 m sedimentary sequence (collected with a Russian peat sampler as 1 m core sections from two overlapping boreholes, correlated via physical sedimentary parameters and coring depth; Lewis, 2011) was retrieved from Kilen from a water depth of 3.9 m (Figure 1c). The lithology of each core section was described using a modified Troels-Smith system (Troels-Smith, 1955; cf. Birks and Birks, 1980), prior to being sliced up into 1 or 2 cm intervals and subsampled for physical sedimentary analyses, micro- and macrofossil analyses plus sedimentary pigment analysis. Organic and calcium carbonate content ($CaCO_3$) was determined for each core slice (from ~1 cm^3 aliquots) via loss-on-ignition (LOI) at 550°C and 925°C respectively (Dean, 1974; Bengtsson and Enell, 1986) following overnight evaporation of interstitial water at 105 °C (also enabling calculation of dry mass and sediment water content). The remaining residue after organic and carbonate LOI forms the minerogenic component of the sediment.

Sedimentary pigments from freeze-dried samples (weighed aliquots of ~0.2-0.4 g from 1-2 cm core slices) were analysed using a modified method of Chen et al., (2001) via high-performance liquid chromatography (HPLC; using an Agilent 1200 series HPLC separation module with Quaternary pump, autosampler, ODS Hypersil column (250 · 4.6 mm; 5 µm particle size), and photo-diode array detector) with two standards per run. Pigments were identified based on their retention time and absorption spectra compared with published literature (e.g. Jeffrey et al., 1997) and commercial standards. All sedimentary and biological assemblages have been zoned via optimal splitting (based on an information content matrix of dissimilarity) using the package PsimPol v. 4.27 (Bennett, 2003-2009), incorporating a broken stick model to test the significance of zone splits. All stratigraphic diagrams were produced using C2 v.1.6.2 (Juggins, 1991-2009).

A total of 521 core slices 1or 2 cm thick were wet-sieved into two fractions (500 µm and 100 µm) and hand-picked for macrofossils, both for obtaining sufficient terrestrial plant material for AMS ^{14}C dating and analysis of molluscs (both fractions) and foraminifera (100 µm fraction). The Kilen chronology is based on 13 AMS ^{14}C dates based on terrestrial plant macrofossil material in order to avoid problems associated with the marine reservoir effect (Heier-Nielsen et al., 1995; Olsen et al., 2009; Philippsen et al., in press). The final age model (Figure 2 and see Philippsen et al., in press) was produced using Oxcal 4.1 (Ramsey, 2008) (k=150, A=73.3%) with the atmospheric calibration curve IntTCal09 (Reimer et al., 2009) and allowances being made for changes in accumulation rate (based on $CaCO_3$ content; Figure 2). Six pollen samples were analysed in order to identify the approximate location of the widespread mid-Holocene *Ulmus* (elm) decline (ca. 5,900 BP; Andersen and Rasmussen, 1993), subsequently providing an independent check on the age model (elm decline dated to ca. 5,850-5,800 BP at Kilen).

For macrofossils (including plants, molluscs and other animals) all distinguishable remains (present from wet sieved fractions) were recorded and, where possible, identified. Mollusc nomenclature follows Petersen (2004).

Diatom samples (taken from 1-2 cm core slices) were prepared using standard techniques outlined in Renberg (1990) and Battarbee et al., (2001) with microspheres being added to assess diatom concentration (after Battarbee and Kneen, 1982) and the diatom flux calculated subsequently based on the age-depth model. A minimum of 300 valves were counted per sample excluding *Chaetoceros* resting spores and *Rhizosolenia* spines. Diatom preservation was assessed using a 2-stage categorization (pristine or dissolved), expressed as an **F**-index ratio (Ryves et al., 2006). Diatom taxonomy was harmonised with the Molten and Define project (http://craticula.ncl.ac.uk/Molten/jsp/; Andrén et al., 2007) for application of the salinity transfer function to fossil diatom data.

Although the original Molten/Define diatom training set was designed primarily as a tool to infer past nutrient (total nitrogen) concentrations in the Baltic Sea, salinity is a major control on diatom composition (see below; Andrén et al., 2007). A subset of 211 sites from the large pan-Baltic Molten/Define modern training set was selected for building a diatom-salinity model that were most appropriate for Danish coastal environments, including Danish, Swedish and Finnish samples, with one site later being removed as an outlier. In this training set, salinity was the most important variable uniquely explaining 7.8% (n = 9999 Monte Carlo permutations, p = 0.0001) in a single-variable analysis and exhibiting little co-variation with other significant variables under variance partitioning (dropping only slightly to 6.6% when total nitrogen, total phosphorus and depth were included as co-variables; n = 9999 permutations, p = 0.0001). Various diatom-salinity transfer functions were developed form this training set, their predictive power tested via bootstrapping (x1000 cycles) and models evaluated using r^2_{boot} and root mean square error of prediction (RMSEP) values (Table 1). A weighted average-partial least squares (WA-PLS) component 2 model was selected as it performed best under internal validation and exhibited a similarly high predictive power to other published salinity-based transfer functions (see Table 1).

Foraminifera assemblage counts (from 2cm core slices) were made on samples using standard techniques described in Feyling-Hanssen et al., (1971) and Knudsen (1998). A minimum of 300 tests were picked identified and counted where possible. Foraminiferal taxonomy follows Ellis and Messina (1949 and supplements). Oxygen and carbon isotopic analyses were performed on tests of *Elphidium excavatum* f. *selseyensis* from 44 samples (~5-20 tests per sample; weight 30-100 µg), using a GV IsoPrime mass spectrometer plus Multiprep device. Isotope values ($\delta^{13}C$, $\delta^{18}O$) are reported as parts per-mille (‰) deviations of the isotopic ratios ($^{13}C/^{12}C$, $^{18}O/^{16}O$) calculated to the VPDB scale using a within-run laboratory standard calibrated against NBS standards. Analytical reproducibility of the standard calcite (KCM) is < 0.1‰ for $\delta^{13}C$ and $\delta^{18}O$. Full details of all methodologies can be found in Lewis (2011).

4. Results and interpretation

4.1. Sediment analyses

4.1.1. Lithology and physical analyses

The profile is composed of near-homogenous grey-brown marine clay gyttja containing varying amounts of silt and sand, plant matter and shell material (Figure 3, see Lewis, 2011 and supplementary data). At the top of the profile higher organic content (Figure 3) is reflected by slightly darker-brown sediment (above 524 cm, ca. 1,900 BP). Based on the physical analyses (organic, $CaCO_3$ and minerogenic matter), three distinct sedimentary zones have been identified (Figure 3), with the lowermost zone (Kil-S1; ca. 7,500-5,000 BP) exhibiting the highest accumulation rates over the study period (~0.33-0.51 cm yr^{-1}). The general pattern of long-term sedimentation at Kilen (i.e. gradually decreasing up the profile) appears typical of the process of shallowing in lakes, where sediment focussing increases the sedimentation rate in deeper parts and declines as the water depth decreases (Hilton, 1985). However, variations in the accumulation of organic, $CaCO_3$ and minerogenic material are visible throughout the profile and likely reflect changing productivity and input of material into the system.

Throughout Kil-S1 organic matter accumulation is relatively high and stable, but there is an almost constant decrease in the accumulation of minerogenic material and, after ca. 7,000 BP a minor decrease in $CaCO_3$. The decrease in all three components (i.e. organic, carbonate and minerogenic matter) between ca. 5,500 and 4,700 BP (marking the Kil-S1 – S2 transition) is probably largely an artefact of sediment focussing. A period of steady sedimentary accumulation occurs after ca. 4,700 BP, before another substantial decline in the accumulation of both minerogenic, and to a lesser degree the organic material after ca. 2,700 BP. The uppermost zone, Kil-S3 (ca.1,900-1,500 BP), is marked by relatively slow (~0.08 cm yr^{-1}), but constant accumulation of all three components.

4.1.2. Sedimentary pigments

A total of 725 samples was analysed over the period ca. 7,500-1,500 BP, yielding eleven identifiable pigments present, together with one ultraviolet absorbing compound (UV-C). Sedimentary pigments are plotted by accumulation (pmol cm^{-2} yr^{-1}) in Figure 3, together with the ultraviolet radiation (UV-R) index (after Leavitt et al., 1997) and pheophytin-*a*/chlorophyll *a* ratio (to assess pigment degradation; e.g. Reuss et al., 2005). The profile has been divided into four statistically significant zones.

In KIL-SP1 (ca. 7,500-6,200 BP) total pigment accumulation is relatively high, with diatoxanthin (from diatoms, dinoflagellates and chrysophytes), lutein (higher plants, green algae, euglenophytes), β-carotene (most algae and plants), pheophytin-*a* (chlorophyll *a* derivative) the most abundant pigment types. A distinct drop in pigment accumulation occurs after ca. 7,100 BP, a pattern which is identifiable in almost all pigments present. However, this decrease is short-lived and soon after ca. 6,800 BP, almost all pigments increase in

abundance again, with the exception of UV-C, which remains present at lower, but variable, levels.

KIL-SP2 (ca. 6,200-5,300 BP) is characterised by high marine productivity as all carotenoid and chlorophyll pigments reach their highest accumulation rates. Lutein, diatoxanthin and β-carotene remain the most individually abundant pigments, while UV-C practically disappears from the record after ca. 6,150 BP. Overall productivity decreases in KIL-SP3 (ca. 5,500-2000 BP) as total pigment accumulation decreases substantially between ca. 5,500-4,700 BP. Thereafter, pigment accumulation remains relatively low, but subject to minor fluctuations throughout the remainder of the profile. In KIL-SP4 (ca. 2,000-1,500 BP), the diatoxanthin accumulation decreases, but alloxanthin (cryptophytes) becomes more abundant. Increased accumulation of lutein, β-carotene, okenone (purple sulfur bacteria), echinenone (cyanobacteria) and the chlorophylls imply slightly elevated productivity levels after ca. 2,000 BP.

4.2. Macrofossils

A total of 521 samples were analysed for macrofossils and concentrations are expressed per 50 ml of wet sediment in Figure 4. Based on the entire macrofossil assemblage (plant macrofossils and molluscs), five statistically significant zones have been identified (Figure 4). Plant macrofossils are generally sparse throughout and with the exception of *Zannichellia palustris* (abundant in Kil-M5), offer little palaeoenvironmental information.

Molluscs were present in 474 samples covering the period ca. 7,500-1,500 BP, at a concentration of up to 125 per 50 ml wet sediment (average 7.3 per 50 ml). Marine bivalves are relatively abundant throughout most of the sequence, characterised by the common inshore 'fjord' type fauna (cf. Petersen, 1981) present in other Limfjord Holocene sequences (e.g. Petersen, 1981; Kristensen et al., 1995). In Kil-M1 (ca. 7,500-6,400 BP), *Corbula gibba* and *Spisula subtruncata* are the most common and abundant mollusc taxa in the Kilen record, supplemented by sporadic occurrences of several other species, particularly *Tellimya ferruginosa* and *Abra alba*. A drop in mollusc concentration occurs in Kil-M2 (ca. 6,400-6,100 BP), as *S. subtruncata* disappears and *C. gibba* decreases in abundance. *Abra alba* is common in Kil-M2, with several occurrences of *Bittium reticulatum* and a peak of *T. ferruginosa* at ca. 6,400 BP.

Mollusc concentration is higher again in Kil-M3 (ca. 6,100-3,750 BP) with *Mysella bidentata* and *A. alba* being the most abundant mollusc species, along with regular occurrences of *T. ferruginosa, Hinia reticulata, S. subtruncata, B. reticulatum* and *Abra* spp.. Another decrease in the mollusc concentration occurs in Kil-M4 (ca. 3,750-2,000 BP) as most taxa become only sporadically present and less abundant. *Abra alba* remains the most regularly recorded species, though *B. reticulatum* is relatively common between ca. 3,000-2,400 BP. A large shift in mollusc composition occurs in the uppermost zone (Kil-M5, ca. 2,000-1,500 BP) as *Parvicardium ovale* becomes more abundant along with a number of low-medium salinity species (including *Hydrobia ventrosa, Hydrobia ulvae, Mytilus edulis, Cerastoderma* spp.

and *Littorina saxatilis*) as overall mollusc concentration reaches its highest Holocene levels at Kilen.

4.3. Diatom assemblages

Kilen diatom assemblages (n = 80; Figure 5) are generally well preserved for marine environments (**F** index = 0.23-0.82; average 0.46; Ryves et al., 2004) and predominately composed of (brackish-) marine benthic and tychoplanktonic diatom taxa, but with planktonic taxa generally being well represented. In Figure 5 the entire diatom assemblage has been divided into three statistically significant zones and is presented alongside a quantitative reconstruction of salinity. Selected diatom-based metrics are also presented in Figure 6.

In KIL-D1 (ca. 7,500-4,700 BP) *Chaetoceros* spp. (8-43 %, average 23 %) are generally most abundant up until ca. 5,400 BP, supplemented by *Opephora mutabilis* (the most abundant benthic taxon), *Paralia sulcata*, *Dimeregramma minor*, and *Grammatophora oceanica*. High-salinity demanding species such as *Delphineis minutissima* and *Cymatosira belgica* briefly appear in the record between ca. 7,000-6,500 BP. After ca. 5,300 BP, *Paralia sulcata* (tychoplanktonic) increases in abundance accompanied by short-term increases in several pelagic taxa including *Skeletonema costatum*, *Cyclotella choctawhatcheeana*, *Cyclotella striata* and *Thalassionema nitzschioides*. These latter taxa generally decline again around ca. 5,400 BP, at roughly the same time as a substantial drop in *Chaetoeceros* resting spores.

Paralia sulcata is the most abundant species throughout KIL-D2 (ca. 4,700-2,000 BP; 14-61 %, average = 35.6 %) as after ca. 4,500 BP percentages of *Chaetoceros* resting spores (and other pelagic taxa) further decrease. *Opephora mutabilis* and *Dimeregramma minor* also decrease in abundance after ca. 3,700 BP as *G. oceanica* briefly becomes the most abundant true benthic taxon (between ca. 3,700-2,600 BP). In the upper section of this zone (after ca. 2,500 BP) *Cymatosira belgica*, *Delphineis minutissima* and the pelagic *Thalassionema nitzschioides* all increase in abundance. In KIL-D3 (ca. 2,000-1,500 BP) high-salinity diatom taxa practically disappear from the record and *Chaetoceros* spp., *Opephora mutabilis* and *Cocconeis scutellum* var. *scutellum* dominate the diatom assemblage. A series of brackish-water periphytic species also appear in the record early in this zone, most notably *Rhoicosphenia abbreviata*, *Epithemia turgida* and *Cocconeis placentula*.

4.5. Benthic foraminifera: assemblages and $\delta^{18}O$ and $\delta^{13}C$ isotopes

The lowermost foraminiferal zone (KIL-F1; ca. 7,400-4,400 BP, Figure 7) is generally characterised by fluctuating abundances of predominately *Elphidium excavatum* f. *selseyensis*, *Elphidium incertum*, *Ammonia beccarii* and *Haynesina germanica*, with smaller abundances of *Elphidium magellanicum*. Highest foraminifera concentrations/fluxes occur at the bottom of the profile (ca. 7,400-6,200 BP), along with maximum diversity and highest percentages of *Haynesina depressula*, *E. magellanicum*, *Stainforthia* sp., and *Bulimina*

marginata. In KIL-F2 (ca. 4,400-2,200 BP) *E. excavatum*, *A. beccarii* and *H. germanica* remain most abundant taxa, but *E. incertum* and *E. magellanicum* both decrease (after ca. 4,700 BP). *Elphidium excavatum* and *H. germanica* both decrease substantially after ca. 3,700 BP, coinciding with an increase in *A. beccarii*. Slightly later (at ca. 2,800 BP), there is a marked increase in *H. germanica*, and it remains a dominant species in the upper part of this zone. *Elphidium williamsoni*, *E. margaritaceum* and *E. gerthi* are also regularly present throughout KIL-F2 at relatively low (but fluctuating) abundances.

A drop in foraminiferal concentration occurs at the onset of KIL-F3 (ca. 2,200-1,900 BP). *Ammonia beccarii* percentages decrease drastically in this zone. *Elphidium excavatum*, *H. germanica* and *E. williamsoni* are the most abundant taxa throughout KIL-F3, though foraminifera remain at low concentrations until ca. 1,900 BP, after which *A. beccarii* increases and *E. margaritaceum*, *E. incertum*, *E. gerthi* and *H. depressula* become present again at low frequencies. After ca. 2,000 BP (Zone KIL-F4; ca. 1,900-1500 BP), foraminifera are again scarce with regularly less than 30 specimens per sample (and absent between ca. 1,600-1,500 BP). Where present, *Elphidium albiumbilicatum* is dominant and *E. williamsoni* and *E. excavatum* are also frequent.

Foraminiferal $\delta^{18}O$ (Figure 7) decreases steadily from +1.7 to +0.4‰ between ca. 6,600 BP and 4,700 BP before increasing abruptly at ca. 4,700 BP and remaining relatively constant up until ca. 3,700 BP. The two samples above this suggest isotopes values decrease again sometime around ca. 2,800 BP. $\delta^{13}C$ fluctuates between –1.1 and –3.0‰ over the period ca. 6,600-4,600 before increasing in the upper section of the profile (–1.2 to –0.4‰ between ca. 4,600-2,500 BP).

5. Discussion

5.1. Marine environmental change at Kilen (ca. 7,500-1,500 BP): regional context

In Figure 8 a summary diagram is provided detailing key multiproxy findings from this study alongside selected regional environmental and climatic parameters. Whilst direct alignment of proxy records must be treated with caution, particularly due to possible dating uncertainties between different sites, there appears to be a close connection between palaeoceanographic changes in the North Sea and Skagerrak with marine environmental change in the western Limfjord. This is exemplified by three apparent shifts in "state" of the Limfjord over the study period ranging from a "state" with stratified waters with high-salinity bottom waters and brackish-marine surface conditions in the lower part of the profile, gradually shifting to a "state" with greater mixing of water column and thus more oceanic sea-surface conditions (high salinity) after ca. 4,400 BP and a change to brackish conditions throughout the water column in the time interval 2,000-1500 BP. These changes appear to be driven by the degree of direct connections between the Limfjord and the North Sea and Skagerrak, for which DI-salinity appears to be a very good proxy, representing relative inputs of fully marine water from the north and west openings.

It is argued that the (diatom, foraminifera and mollusc-based) qualitative interpretation of salinity and quantitative DI-salinity reconstruction presented here are relatively accurate, agreeing well with other published studies in the region in the more recent past (i.e. last, 2,500 years; Kristensen et al., 1995; Christensen et al., 2004, discussed below) and with ecological knowledge of the species present. The importance of salinity in driving trends in the fossil dataset were apparent using detrended correspondence analysis (DCA) using Canoco v.4.5 (ter Braak and Šmilauer, 2002), with fresh/brackish water species falling at opposite ends of DCA axis 1 (explaining 15.7 % of the total variation) to marine species (Lewis, 2011). Goodness-of-fit of the DI-salinity model was assessed for each fossil sample after deleting *Chaetoceros* (resting spores and vegetative cells) by (1) the proportion of fossil diatom data included in the diatom-salinity model and (2) the minimum dissimilarity coefficient between each fossil sample and the training set (Figure 6). Average coverage of fossil data within the diatom-salinity model was 60% (range 37-84%), while analogues scores ranged from 70-113, with a mean of 93, below the threshold range of 100-150 for good analogues suggested by Jones and Juggins (1995); Juggins (2001). Reduced coverage of fossil data within the training set is almost entirely explained by *Chaetoceros* taxa, which generally increase down core. However, no independent test for spatial autocorrelation (Telford and Birks, 2005) was employed in this study and therefore it is acknowledged that performance statistics of the DI-salinity model (Table 1) might be slightly exaggerated due to an element of spatial structuring within the training set.

5.1.1. Kilen phase I, ca. 7,500 to 4,400 BP: deep, productive and stratifying estuary.

5.1.1.1. Environmental change from ca. 7,500 to 6,200 BP

Diatom-inferred salinities (average 25 g L^{-1}, range ~20-31 g L^{-1}) for the late Mesolithic and most of the Neolithic period (ca. 7,500-4,400 BP; Figure 8) generally suggest similar or slightly lower values than at present (ca. 24-27 g L^{-1} at present for the Struer region; Burman and Schmitz, 2005; Hofmeister et al., 2006), despite evidence for higher relative sea levels in the Limfjord (1.5-2 m at Struer; Mertz, 1924) and deeper waters (perhaps 15-20 m deeper at Kilen as suggested by multiproxy evidence in this study) existing during the mid-Holocene. It is therefore argued here that the Limfjord was less open to the west than has been previously suggested (e.g. in palaeo-shoreline estimates; cf. Figure 1b) as any substantially greater opening to the North Sea in the west than at present (~1 km; Figure 1b) is likely to have produced far higher surface salinity (and more oceanic conditions) than suggested by the Kilen diatom record (Figure 5). More localised factors for lower salinity such as increased freshwater input or development of beach ridges/sediment banks (reducing the connection of Kilen with the Limfjord) are deemed unlikely due to the foraminiferal evidence (Figure 7) for high bottom-water salinity existing in Kilen at this time (see below).

The main opening to the Limfjord most likely existed in the north (or north-west), opening into the Skagerrak, as suggested by high reconstructed salinities in the northern Limfjord during the mid-Holocene (Petersen, 1981; Burman and Schmitz, 2005). Obstructive sand banks such as the emergent Jutland Bank (Leth, 1996) might have largely blocked off the

western entrance to the North Sea prior to its drowning sometime around ca. 6,200 BP (Leth, 1996; Gyllencreutz, 2005) and impeded the flow, transport and erosion capacity of the North Jutland current (Figure 1a) thereby enhancing sediment accretion along the western margin of the Limfjord and subsequently reducing water exchange between the Limfjord and the North Sea. A strengthening of the Jutland current and a shift towards coarser sediment in the Skagerrak has been shown to broadly coincide with the drowning of the Jutland Bank (Leth, 1996; Gyllencreutz and Kissel, 2006),

Whilst the diatom assemblage (Figure 5) is largely reflecting salinity in the surface waters and littoral areas, the benthic foraminifera assemblage (Figure 7) suggests that highest bottom-water salinities occurred between ca. 7,400 and 5,000 BP (maxima ca. 7,400-6,900 BP). This is marked by maximum abundances of *Elphidium incertum*, which requires at least 20-24 g L^{-1} and is commonly found in a narrow zone just below the halocline (Lutze, 1965, 1974), *Haynesina depressula* (requiring a minimum of 24 g L^{-1}; Haake, 1962; Alve and Murray, 1999) and presence of *Elphidium magellanicum* and *Bulimina marginata*, which both require relatively high and stable salinity conditions (Murray, 1991; Conradsen et al., 1994). This might imply periodic stratification of the water column, as seen today in areas of the Limfjord (Grooss et al., 1996) and in some of the deeper Danish fjords (e.g. Mariager Fjord), whereby high-salinity oceanic water is overlain by fresher water input at the surface (with salinity differences of up to 6 g L^{-1} recorded between surface and bottom waters in the Limfjord today; Grooss et al., 1996).

It is highly likely that the Kilen basin was deep enough to stratify during the mid-Holocene, with sediment likely accumulating at ~10-15 m below the current lake bed between ca. 7,400-5,400 and with higher relative sea level than present day (Mertz, 1924). This might have enabled the higher salinity demanding foraminifera and mollusc species (e.g. *Tellimya ferruginosa*, *Spisula subtruncata* and *Abra alba*; Figure 4) to live at depth beneath the halocline, and taxa able to tolerate lower salinities (e.g. *Corbula gibba*, *Hydrobia ulvae*) to occupy the surface waters or shallower, lower salinity (i.e. more regularly mixed) areas of the fjord. Deep water with regular stratification is further supported by the high percentage of pelagic diatom taxa (particularly *Chaetoceros* resting spores; Figure 5), presence of deep-water favouring foraminifera (such as *Buliminia marginata*, Figure 7; cf. Murray, 1991) and the relatively high abundance of okenone, produced by planktonic purple sulfur bacteria that live in anoxic conditions (Figure 3).

$\delta^{18}O$ values are also interpreted as a proxy for bottom-water salinity up until ca. 4,600 BP (Figure 7), and in agreement with the foraminifera data they suggest relatively high salinity between ca. 6,600-4,600 BP (high $\delta^{18}O$), though characterised by a gradual freshening of the bottom water (decreasing $\delta^{18}O$), likely due to decreasing regularity of stratification as the fjord becomes progressively shallower (resulting from high sedimentation rates (Figure 3) and sea level decline (after ca. 6,000 BP) due to isostatic rebound). Low $\delta^{13}C$ (below 'typical' marine values of ~0‰; Sharp, 2007) between ca. 6,600-4,600 BP (Figure 7) probably indicate that foraminifera utilising greater respired/mineralised carbon dioxide (CO_2) under stratified conditions.

Sea-level change in the western Limfjord is extremely complicated and poorly understood, particularly due to variable rates of isostatic rebound across the Limfjord (e.g. Petersen, 1981; Gehrels et al., 2006), with the study site being very close to the isostatic 'hinge point' between the uplifting and subsiding regions, which itself has migrated through time (Gehrels et al., 2006). The only available sea level curves are from southwest Denmark (e.g. Gehrels et al., 2006; Pedersen et al., 2009) within the subsidence zone, where relative sea level has been rising over the study period and to the north, where uplift has caused relative sea level decline since about 5,900 BP (e.g. Petersen, 1981), neither of which can be directly applied to SW Limfjord.

It is likely that the sea level in the Kilen area reached its maximum height of~1.5-2 m above present (Mertz, 1924) sometime in the Late Mesolithic (cf. Petersen, 1981; Berglund et al., 2005) and has been largely declining since then, though whether any of the transgressive/regressive phases seen across Denmark and the Baltic Sea (e.g. Berglund et al., 2005) are identifiable in the south western Limfjord remains uncertain. In terms of salinity (and productivity), sea level (and subsequent exposure to the North Sea and Skagerrak) is clearly an important driver, though the level of connection of the Limfjord with the open seas is further complicated by changing coastal geomorphology (i.e. building up of coastal spits and sand barriers) and climate change, particularly storminess associated with atmospheric pressure systems (e.g. North Atlantic Oscillation (NAO); see below).

High pigment concentrations and organic matter content between ca. 7,400 and 7,000 BP (Figure 3) suggests that the productivity was relatively high at the bottom of the profile, coinciding with the highest Holocene temperatures in Scandinavia (Holocene Thermal Maximum (HTM); Snowball et al., 2004; Antonsson and Seppä, 2007; Seppä et al., 2009; Brown et al., 2012; Figure 8). There is, however, a brief decrease in pigment accumulation rates between ca. 7,000-6,800 BP, which coincides with increased DI-salinities (>28 g L^{-1}; Figure 5) and the first major reduction in pelagic diatom taxa (P1; Figure 6). This might be the result of increased input of saline water from the North Sea/Skagerrak, perhaps during stormier conditions (e.g. Yu, 2003; Yu and Berglund, 2007 and see below) or alternatively might be related to a short-term reduction in freshwater input to Kilen, supplying nutrients as well, and possibly causing a breakdown in stratification.

The high abundance of UV-C between ca. 7,400 and 6,200 BP (Figure 3), suggests increased depth penetration of UV-radiation (Leavitt et al., 1997). UVR pigments are primarily produced by benthic sediment dwelling organisms (e.g. cyanobacteria) as photo-protectants when subjected to increased UV-exposure (Leavitt et al., 1997; McGowan, 2007). Dissolved organic carbon (DOC) is important in aquatic systems for shading out UV-radiation (e.g. Scully and Lean, 1994; Leavitt et al., 1997) which might suggest that DOC levels were lower before ca. 6,200 BP, and protective pigmentation was needed despite the likely greater light shading from a deep, turbid water column with high minerogenic content and significant algal biomass (Figure 3). Plenty of light penetration and low DOC is further supported by the presence of purple sulfur bacteria (indicated by okenone in the pigment record; Figure 3), which exist under anoxic conditions, often in highly productive systems, but when light can

still reach the deeper water layers (i.e. clear water). Okenone is therefore often used to infer stratification in limnic and coastal systems (Smittenberg et al., 2004; McGowan, 2007).

5.1.1.2. Environmental change from ca. 6,200 to 4,400 BP

A high productivity phase occurs between ca. 6,200 and 4,900 BP, marked by a high organic matter content and increased accumulation of sedimentary pigments (Figure 3) and diatoms (including an increased presence of pelagic diatom taxa; Figure 6). There is also a striking disappearance of UV-C after ca. 6,200 BP, most likely due to internal loading of DOC from phytoplankton blooming (Mannino and Harvey, 2000) and direct shading by phytoplankton, reducing the UV-penetration within the fjord, at least to the benthic areas. The increase in okenone after ca. 6,300 BP (Figure 3) suggests that light still penetrated into the stratified anoxic layers. Progressive shallowing of the basin (especially after ca. 5,400 BP) might also have increased turbidity.

The fact that UV-C is not found in the Kilen sequence even after this productivity maximum (ending ~4,900 BP; Figure 3), by which time Kilen was shallower and less productive (and therefore probably experienced greater benthic UV exposure), would accord with a deep-water benthic habitat for the organism(s) responsible for these pigments, although sediment re-suspension and turbidity would also increase with lower water level, perhaps also limiting purple sulfur bacteria (i.e. low okenone accumulation after ca. 5,000 BP) . Increased input of terrestrially sourced DOC, perhaps associated with catchment changes such as forest restructuring following the *Ulmus* decline and the introduction of agriculture (ca. 5,900 BP; Andersen and Rasmussen, 1993), might also have helped to block out UV-radiation.

Accordingly, high productivity between ca. 6,200 and 5,800 BP (Figure 3) is most likely the result of changes in the marine environment, rather than changing inputs from terrestrial sources. Stratification is still prevailing, as indicated by the foraminifera (Figure 7), and might even have intensified (i.e. become more regular as exemplified by both high pigment fluxes and increased diatom plankton) following the drowning of the Jutland Bank (ca. 6,200 BP; Leth, 1996; Gyllencreutz and Kissel, 2006) and likely opening (or widening) of the western Limfjord connection to the North Sea. Subsequently, nutrient recycling might have become more intense under increasingly more stratified conditions, resulting in higher productivity and enabling nutrient-demanding planktonic organisms (e.g. diatoms; *Chaetoceros* resting spores, *Cyclotella choctawhatcheeana*, *C. striata*, *Skeletonema costatum*; Figure 5) and bacterioplankton to bloom. This might in turn induce greater production of DOC and reduce UV-light penetration to the benthic areas. A prolonged period of high productivity in the Limfjord might have been sustainable due to regular input of highly saline, oxygenated water through the northern and western openings (encouraging stratification of water masses), perhaps associated with increased storminess (as evident in the GISP2 ice core record between ca. 6000-5,000 BP (Mayewski et al., 1997) and linked to sea level events in the Baltic Sea (Yu, 2003; Yu and Berglund, 2007) and subsequently increased erosion along the Limfjord coastline.

A secondary increase in sedimentary pigment concentrations occurs ca. 5,800 BP (Figure 3), which might suggest a later role for terrestrial input of nutrients following human activities

(e.g. induced by early forest clearance) as evident in numerous terrestrial pollen records (e.g. Iversen, 1941; Aaby, 1986; Odgaard, 1994; Andersen, 1995b; Rasmussen, 2005). In the palynological record, elevated abundances of Poaceae pollen at ca. 5,800 BP, and shortly after the appearance of *Plantago lanceolata* (ribwort plantain), marks the first signs of major agriculture-based land-use changes in the Kilen area (P. Rasmussen, unpublished data). This interpretation must, however, be treated with caution due to the low number of pollen analyses at Kilen, but would be in good agreement with other Danish palynological studies (Aaby, 1986; Odgaard, 1989, 1994; Rasmussen, 2005).

After a brief drop, DI-salinity begins to rise again after ca. 5,200 BP, reaching near fully marine sea-surface conditions (>30 g L^{-1}) shortly after ca. 4,200 BP (Figure 5). The foraminifera suggest that the seasonal stratification of the water column ceased after ca. 4,400 BP and that the water column was mixed during the remaining part of the record. Whilst, the $\delta^{18}O$ suggest an increase in salinity after ca. 4,600 BP (marked by a ~0.8‰ increase in $\delta^{18}O$; Figure 7), again probably reflecting the shift to mixed water conditions (i.e. absent or rare stratification), after which $\delta^{18}O$ become a proxy of overall water column salinity, rather than bottom-water salinity only.

The reduction in organic matter, flux of sedimentary pigments (Figure 3) and decline in pelagic diatom abundance (i.e. second major reduction in pelagic diatom taxa, P2; Figure 6, particularly *Chaetoceros* resting spores; Figure 5) suggest a decline in marine primary productivity after ca. 5,400 BP. This might signify reduced stratification (supported by low okenone abundance after ca. 5,000 BP) due to continuous shallowing of the Kilen basin caused by both sediment accumulation and isostatic land uplift. There is little change in the pheophytin-*a*/chlorophyll *a* ratio, which suggests that poorer preservation is not responsible for this drop in pigment concentrations (Figure 3). After ca. 4,800 BP, the sedimentary pigment concentration and accumulation rates generally remain relatively low. Increased energy in the system (due to stronger currents, increased exposure and shallower depth) as marine conditions intensified at Kilen (after ca. 5,000 BP), might also have caused greater transportation, re-working and re-deposition of sediments out of the Kilen basin and poorer preservation (e.g. lower plant macrofossil and mollusc concentration (Figure 4), lower diatom **F** index; (Figure 6)).

5.1.2. Phase II, ca. 4,400-2,000 BP: non stratified, high salinity oceanic estuary

Diatom-inferred salinities gradually rise throughout the Bronze Age and the early Iron Age perhaps due to gradual widening of the western Limfjord opening, though the overall assemblage indicates that Kilen became a shallow, benthic dominated system from ca. 4,400 BP, completing a process that began perhaps a thousand years before, although the final stage was rapid. This third major drop in pelagic diatom taxa (P3, Figure 6), and an increase in foraminifera indicative of shallow intertidal conditions, particularly *Elphidium williamsoni* (Figure 7; cf. Alve and Murray, 1999) likely marks the end of any stratification, as the Kilen basin becomes too shallow to prevent mixing of water masses.

The foraminiferal assemblage suggests a transitional phase between ca. 4,400 and 3,600 BP following the termination of stratified conditions within the basin and subsequent mixing of the water column, as indicated by the remaining relatively high contents of *Elphidium excavatum* (Figure 7). Gradually more unstable conditions prevail between ca. 3,700 and 2,800 BP, although with relatively high salinity being inferred by the presence of foraminiferal taxa such as *E. magellanicum* and *E. margaritaceum*. Both the diatom and foraminiferal assemblages document a salinity decline around 2,800 BP, where the subtidal euryhaline species *Haynesina germanica* (cf. Murray, 1991) become dominant and the intertidal *E. williamsoni* appears. This might be related to a globally synchronous, solar-forced climatic event occurring ca. 2,800 years ago, which manifested itself as a cooler and wetter phase in northwest European sediment records (Martin-Puertas et al., 2012), or a sea-level decline reducing the input of marine water from the North Sea, though no reliable record of sea-level change exists for the SW Limfjord during this period. $\delta^{18}O$ values remain relatively stable after ca. 4,600 BP (Figure 7), with the exception of a decline at ca. 2,500 BP, which might represent a rapid freshwater input event, though as this is not identifiable in any other proxies might be a response to some other variable (e.g. test dissolution), or reworking. The $\delta^{13}C$ increase by ~0.5-1‰ after ca. 4,600 BP (Figure 7), is likely due to greater mixing with open marine water following reduced stratification and greater input of normal marine salinity waters from the North Sea (as marked by increasing DI-salinity). Therefore, overall the rather limited isotope data set (particularly after ca. 4,500 BP) support the foraminiferal assemblage counts and other proxy data for changes in stratification state.

Ammonia beccarii is a dominant species accounting for >40 % of the fauna between ca. 3,600 and 2,300 BP (Figure 7). This species is found today both in brackish waters (Walton and Sloan, 1990; Murray, 2006) and in fully marine waters (Rouvillois, 1970; Alve and Murray, 1999) and in the Kilen sequence, it appears to become dominant during the transitional phase of mixed water, corresponding to its present-day distribution in Danish marginal marine environments (Alve and Murray, 1999).

The high abundances of *Paralia sulcata* and *Grammatophora oceanica* (Figure 5) and regular presence of high-salinity demanding mollusc taxa (i.e. *Bittium reticulatum, Abra alba*; Figure 4) suggests that near fully marine conditions existed at Kilen at this time. It is argued here that in this section of the profile (i.e. between ca. 4,400-2,300 BP) the diatoms and molluscs are more accurately reflecting the salinity pattern (i.e. increasing salinity reaching near fully marine conditions), though it is acknowledged that the DI-salinity values are over-estimated in some samples between ca. 2,300-2,000 BP (see below), whilst the foraminifera must be responding to some other variable, possibly decreasing water depth as the benthic habitat becomes more restricted (e.g. decreased living space, increased competition for resources), or are being heavily affected by test dissolution, apparent in samples after ca. 4,400 BP.

After ca. 2,800 BP, DI-salinity increases again reaching maximum Holocene levels between ca. 2,500 and 2,000 BP, at which point the assemblage is dominated by high-salinity demanding species such as *Paralia sulcata*, *Cymatosira belgica* and *Delphineis minutissima* (Figure 5). A slight increase in *Elphidium excavatum* (indicative of open water conditions), together with *E. incertum* and *E. magellanicum* in the foraminiferal record between ca. 2,100

and 2,000 BP support increased salinity in the late Pre-Roman period, whilst maximum abundances of *E. williamsoni* indicates a further decrease in water depth (Figure 7). This salinity maximimum is likely to mark the maximum connection of the western Limfjord with the North Sea and presumably also implies that a connection still existed with the Skagerrak to the north.

Higher sea levels might explain this period of higher salinity, perhaps due a period of increased storminess causing piling up (and subsequently greater input) of high-salinity sea water in east North Sea and Baltic Sea, similar to the prolonged NAO+ type cycles identified by Yu and Berglund (2007), though the long-term history of the NAO remains uncertain and only tentative links can be made here. Nevertheless, high salinity is documented at the more northerly Bjørnsholm Bay site around 2,200-2,800 BP (Christensen et al., 2004; Mertens et al., 2011), suggesting that a connection between the Limfjord and the Skagerrak existed at this time, despite long-term sea-level decline occurring in the northern region due to isostatic uplift (Petersen, 1981). Higher summer and winter temperatures, inferred by regional pollen reconstructions (Antonsson and Seppä, 2007; Seppä et al., 2009; Brown et al., 2012; Figure 8) and drier conditions, inferred from several Danish and Swedish peat and lake records (e.g. Barber et al., 2004; Olsen et al., 2010), possibly indicate that greater evaporation and reduced freshwater input from the catchment during the Pre-Roman Iron Age might also be important for explaining near-fully marine salinities between ca. 2,500 and 2,000 BP (Figure 8).

In several of the more poorly preserved samples (**F**<0.4, Figure 6), exceptionally high salinities (35-43 g L^{-1}) are inferred, even exceeding present day average salinities for fully marine conditions (i.e. > 35 g L^{-1}). However, even during maximum exposure to the North Sea, the salinity of the Limfjord is unlikely to exceed 35 g L^{-1} and therefore we conclude salinity has been over-estimated by the model in this section of the record ca. 2,300-2,000 BP. Poor preservation has been linked elsewhere in the Limfjord and in inland saline lakes, to overestimation of DI-salinity (Ryves et al., 2004; Ryves et al., 2006). Nevertheless, (as indicated above) almost fully marine salinities in the late Pre-Roman Iron Age are consistent with foraminiferal, dinoflagellate and mollusc records from the Bjørnsholm Bay region (Kristensen et al., 1995; Christensen et al., 2004; Mertens et al., 2011) and also with high salinity inferred from diatoms and molluscs at Horsens Fjord, East Jutland and Tempelkrog in Isefjord, Zealand (D.B.Ryves et al., unpublished data). Despite this, overall the application of the diatom-salinity model is considered to have produced a reliable reconstruction of salinity change over the study period (further supported by C/N and $\delta^{13}C$ analyses on bulk sediment from Kilen; Philippsen et al., in press) that can also be qualitatively confirmed by ecological knowledge. Existing palaeosalinity inferences for the Limfjord are only available for the last ca. 2,800 years, over which period the Kilen DI-salinity record is in relatively good agreement with other published records of salinity change (e.g. Christensen et al., 2004; Mertens et al., 2011).

5.1.3. Kilen phase III, ca. 2,000-1500 BP: shallow brackish lagoon

A marked shift to brackish conditions occur around 2,000 BP, with DI-salinity falling by over 10 g L^{-1} (~19.9 g L^{-1} at ca. 1,900 BP; Figure 8). The high-salinity diatoms such as

Cymatosira belgica and *Delphoneis minutissima* practically disappear from the record, and *Paralia sulcata* abundance drops substantially, as brackish-marine species such as *Opephora mutabilis* and *Cocconeis scutellum* become more abundant in the record (Figure 5). This is further supported by an increase in the abundance of brackish water molluscan taxa (e.g. *Mytilus edulis*, *Hydrobia ventrosa*, *Hydrobia ulvae*, *Cerastoderma* spp.; Figure 4) and the regular presence of *Zannichellia palustris* (horned pondweed; Figure 4) after ca. 2,000 BP, which only grow in brackish-water with an upper salinity tolerance of 12-15 g L^{-1} (Moeslund et al., 1990).

After 2,000 BP, the foraminiferal assemblage is seriously affected by dissolution of tests, but when present, dominance of *Elphidium albiumbilicatum* supports brackish-water conditions at this time (Figure 7). This species tolerates salinity as low as 3 g L^{-1}, but the presence of additional species such as *E. excavatum*, *E. williamsoni* and *Haynesina germanica*) suggests that salinity did not fall below 15 g L^{-1}. The cause of this salinity decline is likely to be a closing, or at least severe narrowing, of both the northern (seen also in the central Limfjord; Kristensen et al., 1995; Christensen et al., 2004) and western openings of the Limfjord, probably due to greater accretion of sediments (building up spits and sand barriers), driven by climate change (Clemmensen et al., 2009) and/or sea-level decline due to isostatic uplift (Petersen, 1981).

In addition to long-term deposition of sediments transported from the west by the Jutland Current and re-deposited along the Jutland-Skagerrak coastline (Jiang et al., 1997; Gyllencreutz and Kissel, 2006), this closure also broadly coincides with a period of increased aeolian activity and subsequent dune building along the northwestern and northern coasts of Jutland (Clemmensen et al., 2009). The initiation of these aeolian events (indicated on Figure 8) has been linked to wet/cool summers (in Swedish peat bog records) and are believed to represent more frequent passage of cyclones across Denmark in the summer season (Clemmensen et al., 2009). Increased freshwater input to the Limfjord might have lowered salinity, whilst increased storminess and movement of aeolian material probably contributed to the closure of the Limfjord's entrances (via sedimentary accretion) to the North Sea and Skagerrak.

There is some evidence for increased marine productivity in the Roman period with both mollusc and plant macrofossil concentrations increasing after ca. 2,000 BP. Total pigment accumulation also increases slightly after ca. 1,900 BP (Figure 3), driven by specific sedimentary pigments, most notably alloxanthin (from cryptophytes), lutein (from green algae, euglenophytes, higher plants) and canthaxanthin (from colonial cyanobacteria). In contrast to this, diatoxanthin (from diatoms, dinoflagellates and chrysophytes) and the diatom concentration/flux (Figure 6) decrease around the onset of the Roman period (ca. 2,000-1,500 BP) and remain low thereafter. This decrease might be explained by a decline in silica supply, increased competition for resources from other algal groups or greater predation of diatoxanthin-producing communities by molluscs, ostracods (both of which increase in abundance in the brackish Roman period) and other higher organisms.

5.2. Interactions between environment and society

Shell middens are relatively common archaeological sites across coastal Denmark, but somewhat surprisingly are absent from the western Limfjord (see Figure 1b) throughout the entire Holocene (Andersen, 1992a; Andersen, 1995a, 2000b, 2007). For the late Mesolithic/early Neolithic period, lower surface salinity in the western Limfjord might explain this absence, with regular stratification likely preventing high-salinity water from reaching the innermost, shallow areas of fjords and estuaries, thereby restricting the heavily exploited, high-salinity demanding oysters (abundant in the Mesolithic layers of shell middens throughout Denmark; Andersen, 2007) to the deeper, inaccessible waters. High sedimentary accumulation rates during the Ertebølle period (e.g. 0.36-0.51 cm^{-2} yr^{-1}; 7,400-5,800 BP) might also be important for preventing oyster colonisation and establishment of beds. *Ostrea edulis* struggles with higher volumes of fine sediment, being less efficient at ejecting continuously accumulating sediment from its mantle cavity than species such as *Cerastoderma edule* (Yonge, 1960; Bailey and Milner, 2008).

The widely observed oyster decline in shell middens across Denmark at the Mesolithic-Neolithic transition (ca. 5,900 BP) has encouraged the development of a geographically widespread model to explain this shift, with a decline in salinity being the most commonly cited, single causal factor (Rowley-Conwy, 1984; Andersen, 2007; cf. Schulting, 2010). Archaeologically, this model has already been challenged by inconsistencies in other shell middens, such as Krabbesholm and Visborg, both of which contain Neolithic layers in which oysters remain abundant (Andersen, 2000a, 2005; Nielsen, 2008). Here, it can be challenged by environmental data from the western Limfjord (Figure 4-7), which directly contradicts the hypothesis that lower salinity existed across the Limfjord during the early Neolithic period. Similarly, a decline in salinity is also unable to explain the oyster decline in the Norsminde Fjord shell midden (east Jutland) and subsequently a sedimentary hypothesis is proposed for this site (Lewis, 2011). It is likely that more localised factors, dependent upon catchment characteristics (cf. Nielsen, 2008; Lewis, 2011) might be more important than previously thought. In future, propagation of regional environmental changes into individual fjord and estuarine systems from common forcing factors such as sea level and climate change must be considered more closely and critically tested by local palaeodata (Lewis, 2011).

In the Bronze Age (3,600-2,400 BP), marine resources were still exploited (e.g. occasional shell layers and fishing tools and artefacts; Rasmussen, 1992; Andersen, 1998; Ringtved, 1998) but appear to be much less important and coastal shell middens are absent from the entire Limfjord (Andersen, 2007). This study suggests that higher salinity conditions, and generally lower marine productivity (i.e. lower pigment fluxes) existed in the Bronze Age (Figure 8), likely accompanied by greater energy and currents and coarser sediment, which might have limited or confined natural shell beds to specific areas of the Limfjord.

Shoreline shell middens are also absent from the entire Limfjord throughout the Iron Age (2,400-900 BP), though this is somewhat aberrant and difficult to explain (large shell middens predominately composed of the blue mussel (*Mytilus edulis*) are abundant along the east coast of Jutland, concentrated between ca. 2,300 and 1,700 BP; Poulsen, 1978; Andersen, 2007). Regional molluscan records document that *Mytilus edulis* was present in the Limfjord during the Roman period (Kristensen et al., 1995; this study) ruling out absence of

this resource. The high abundance and widespread spatial distribution of mussels during the Iron Age might have meant that site selection was more heavily determined by additional resources available to these cultures. Alternatively mussels might have been collected more sporadically (perhaps as a dietary supplement), from different localities, preventing significant accumulation of shell middens: a number of sites have been found several kilometres inland, containing heaps of marine molluscs or smaller shell middens (Mikkelsen, 1994; Andersen, 2007), while some existing data indicate small numbers of shells were transported to more inland settlement sites prior to shelling (Poulsen, 1978; Ringtved, 1992).

6. Conclusions

This high-resolution study of Kilen has provided new and detailed information about the environmental history of the western Limfjord, much of which can be extrapolated to the Limfjord proper, with three major salinity and productivity shifts being documented between ca. 7,500 and 1,500 BP. Kilen in phase I (ca. 7,500-4,400 BP) was a brackish-marine estuary with high productivity and regular stratification of water masses. There was a gradual transition to phase II, which was characterised by near fully marine salinities, low productivity and shallow water (probably encouraging greater mixing of water masses and ending stratification of the basin), and then a sudden switch to brackish conditions with medium-low productivity in phase III (between ca. 2,000-1,500 BP), likely in response to the previously documented Iron Age closure of the Limfjord. These shifts can be (broadly) synchronously linked to palaeoceanographic events registered in the North Sea and Skagerrak (e.g. drowning of the Jutland Bank) and to climate change in northern Europe. Of particular importance is the relative exposure of the Limfjord to these two seas (North Sea and Skagerrak), which appears to be driven by a complex interplay between climate, sea level, ocean currents, erosion and sedimentary accretion along the outer margin of the Limfjord.

Overall, the data here indicate that the Limfjord is a fragile system, subject to large scale changes in ecosystem structure and physical conditions over a range of timescales. Importantly, this study has provided a high-resolution, well dated multiproxy record of environmental change from an important archaeological region, enabling future debate concerning links between sea and society to be placed within a proper environmental context.

7. Acknowledgments

Beth Stavngaard, Ole Bennike and Bent Odgaard are thanked for field and laboratory support. Molten and Define members are also thanked for transfer function production, support and helpful comments and discussion. Funding from Loughborough University Development Fund (Ph.D. funding for JPL), Quaternary Research Association (QRA) New Researchers' Award (for sedimentary pigments to JPL) and NERC Isotope Geosciences Facilities Steering Committee (NIGFSC; award no. IP/1080/1108, for isotope analysis to

DBR and JPL) and the Geological Survey of Denmark and Greenland (for funding several ^{14}C-datings) are gratefully acknowledged. Two anonymous reviewers are thanked for thorough and thoughtful reviews that have improved the paper. This manuscript is dedicated to Kaj Strand Petersen, who sadly passed away during the course of this project and will be greatly missed by family, friends and colleagues.

8. References

Aaby, B., 1986. Trees as anthropogenic indicators in regional pollen diagrams from eastern Denmark. In: Behre, K.E. (Ed.), Anthropogenic indicators in pollen diagrams. Balkema, Rotterdam, pp. 73–93.

Alve, E., Murray, J.W., 1999. Marginal marine environments of the Skagerrak and Kattegat: a baseline study of living (stained) benthic foraminiferal ecology. Palaeogeography, Palaeoclimatology, Palaeoecology 146, 171–193.

Andersen, B., 1992a. En undersøgelse af holocæne foraminiferfaunaer fra Vilsund i det vestlige Limfjordsområde. Dansk Geologisk Forening, Årsskrift for 1990-1991, 47–52.

Andersen, S.H., 1992b. Marin udnyttelse af Limfjorden i stenalderen. Limfjordsprojeket. Rapport nr. 4: Limfjordsfiskeri i fortid og nutid, pp. 65-96.

Andersen, S.H., 1995a. Coastal adaption and marine exploitation in Late Mesolithic Denmark - with special emphasis on the Limfjord region. In: Fischer, A. (Ed.), Man and Sea in the Mesolithic. Coastal settlement above and below present sea-level. Oxbow Books, Oxford, pp. 41-66.

Andersen, S.H., 1998. Erhvervsspecialisering og ressourceudnyttelse i Limfjordsområdet i forhistorisk tid. Limfjordsprojektet: Variation og enhed omkring Limfjorden, Rapport nr. 8, 97-139.

Andersen, S.H., 2000a. Fisker og bonde ved Visborg. In: Hvass, S. (Ed.), Vor skjulte kulturarv. Arkæologi under overfladen. Det Kongelige Nordiske Oldskriftselskab/Jysk Arkæologisk Selskab, Højbjerg. Pp. 42-43

Andersen, S.H., 2000b. 'Køkkenmøddinger' (shell middens) in Denmark: a survey. Proceedings of the Prehistoric Society 66, 361–384.

Andersen, S.H., 2005. Køkkenmøddingerne ved Krabbesholm. Ny forskning i stenalderens kystbopladser. Nationalmuseets Arbejdsmark. pp. 151-171.

Andersen, S.H., 2007. Shell middens ("Køkkenmøddinger") in Danish prehistory as a reflection of the marine environment. In: Milner, N., Craig, O.E., Bailey, G.N. (Eds.), Shell Middens in Atlantic Europe, Oxbow Books, Oxford, pp. 31–45.

Andersen, S.H., Johansen, E., 1986. Ertebølle revisited. Journal of Danish Archaeology 5, 31–61.

Andersen, S.T., Rasmussen, K.L., 1993. Radiocarbon wiggle-dating of elm declines in northwest Denmark and their significance. Vegetation History and Archaeobotany 2, 125–135.

Andersen, S.T., 1995b. History of vegetation and agriculture at Huse Mose, Thy, Northwest Denmark, since the Ice Age. Journal of Danish Archaeology 118, 57–79.

Andrén, E., Clarke, A.L., Telford, R.J., Weckström, K., Vilbaste, S., Aigars, J., Conley, D., Johnsen, T., Juggins, S., Korhola, A., 2007. Defining reference conditions for coastal areas in the Baltic Sea. TemaNord 583, pp. 81.

Antonsson, K., Seppä, H., 2007. Holocene temperatures in Bohuslän, southwest Sweden: a quantitative reconstruction from fossil pollen data. Boreas 36, 400–410.

827 Bailey, G., Milner, N., 2008. Molluscan archives from European prehistory. In: Antczack, A.,
828 Cipriani, R. (Eds.), Early Human Impacts on Megamolluscs, BAR International
829 Series, 165, 111-134.
830 Barber, K.E., Chambers, F.M., Maddy, D., 2004. Late Holocene climatic history of northern
831 Germany and Denmark: peat macrofossil investigations at Dosenmoor, Schleswig-
832 Holstein, and Svanemose, Jutland. Boreas 33, 132–144.
833 Battarbee, R.W., Kneen, M.J., 1982. The use of electronically counted microspheres in
834 absolute diatom analysis. Limnology and Oceanography 27, 184–188.
835 Battarbee, R.W., Carvalho, L., Jones, V.J., Flower, R.J., Cameron, N.G., Bennion, H.,
836 Juggins, S., 2001. Diatoms. In: Smol, J.P., Birks, H.J.B., Last, W.M. (Eds.), Tracking
837 environmental change using lake sediments. Volume 3: Terrestrial, algal, and
838 siliceous Indicators, Kluwer Academic Publishers, Dordrecht, pp. 155-202.
839 Bengtsson, L., Enell, M., 1986. Chemical Analysis. In: Berglund, B.E. (Ed.), Handbook of
840 Holocene palaeoecology and palaeohydrology. John Wiley & Sons, Chichester, New
841 York, pp. 423–451.
842 Bennett, K.D., 2003-2009. Psimpoll. http://www.chrono.qub.ac.uk/psimpoll/psimpoll.html.
843 Berglund, B.E., Sandgren, P., Barnekow, L., Hannon, G., Jiang, H., Skog, G., Yu, S.Y., 2005.
844 Early Holocene history of the Baltic Sea, as reflected in coastal sediments in
845 Blekinge, southeastern Sweden. Quaternary International 130, 111–139.
846 Birks, H.J.B., Birks, H.H., 1980. Quaternary Palaeoecology. Edward Arnold, London, UK.
847 Brown, K.J., Seppä, H., Schoups, G., Fausto, R., Rasmussen, P., Birks, H.J.B., 2012. A
848 spatio-temporal reconstruction of Holocene temperature change in southern
849 Scandinavia. The Holocene 22, 165–177.
850 Burman, J., Schmitz, B., 2005. Periwinkle (*Littorina littorea*) intrashell delta $\delta^{18}O$ and delta
851 $\delta^{13}C$ records from the mid-Holocene Limfjord region, Denmark: a new high-
852 resolution palaeoenvironmental proxy approach. The Holocene 15, 567–575.
853 Chen, N., Bianchi, T.S., McKee, B.A., Bland, J.M. 2001. Historical trends of hypoxia on
854 Louisiana shelf: application of pigments as biomarkers. Organic Geochemistry 32,
855 543–561.
856 Christensen, J.T., Cedhagen, T., Hylleberg, J., 2004. Late-Holocene salinity changes in
857 Limfjorden, Denmark. Sarsia 89, 379–387.
858 Clemmensen, L.B., Murray, A., Heinrich, D., de Jong, R., 2009. The evolution of Holocene
859 coastal dunefields, Jutland, Denmark: a record of climate change over the past 5000
860 years. Geomorphology 105, 303–313.
861 Conley, D.J., Bjorck, S., Bonsdorff, E., Carstensen, J., Destouni, G., Gustafsson, B.G.,
862 Hietanen, S., Kortekaas, M., Kuosa, H., Meier, H.E.M., Muller-Karulis, B., Nordberg,
863 K., Norkko, A., Nurnberg, G., Pitkanen, H., Rabalais, N.N., Rosenberg, R., Savchuk,
864 O.P., Slomp, C.P., Voss, M., Wulff, F., Zillen, L., 2009. Hypoxia-related processes in
865 the Baltic Sea. Environmental Science & Technology 43, 3412–3420.
866 Conradsen, K., Bergsten, H., Knudsen, K. L., Nordberg, K., Seidenkrantz, M.-S., 1994.
867 Recent foraminiferal distribution in the Kattegat and the Skagerrak, Scandinavia.
868 Cushman Foundation for Foraminiferal Research, Special Publication 32, 53–68.
869 Dean, W.E., 1974. Determination of carbonate and organic-matter in calcareous sediments
870 and sedimentary-rocks by loss on ignition - comparison with other methods. Journal
871 of Sedimentary Petrology 44, 242–248.
872 Ellis, B.F., Messina, A., 1949. Catalogue of Foraminifera (Supplements, including 2007).
873 American Museum of Natural History and Micropaleontology Press, New York.
874 Enghoff, I.B., 1999. Fishing in the Baltic region from the 5th century BC to the 16th century
875 AD: evidence from fish bones. Archaeofauna 8, 41–85.

Enghoff, I.B., 2011. Regionality and biotope exploitation in Danish Ertebølle and adjoining periods. The Royal Danish Academy of Sciences and Letters, Scientia Danica. Series B, Biologica 1.

Enghoff, I.B., MacKenzie, B.R., Nielsen, E.E., 2007. The Danish fish fauna during the warm Atlantic period (ca. 7000-3900 BC): Forerunner of future changes? Fisheries Research 87, 167–180.

Feyling-Hanssen, R.W., Jørgensen, J.A., Knudsen, K.L., Lykke-Andersen, A.-L., 1971. Late Quaternary foraminifera from Vendsyssel, Denmark and Sandnes, Norway. Bulletin of the Geological Society of Denmark 21, 1–317.

Fischer, A., Kristiansen, K., 2002. The Neolithisation of Denmark. 150 years of debate. J.R.Collis, Sheffield.

Gehrels, W.R., Szkornik, K., Bartholdy, J., Kirby, J.R., Bradley, S.L., Marshall, W.A., Heinemeier, J., Pedersen, J.B.T., 2006. Late Holocene sea-level changes and isostasy in western Denmark. Quaternary Research 66, 288–302.

Grooss, J., Laursen, M., Deding, J., Jensen, B., Larsen, F., Platz, E.-M., Bendtsen, S.A., Rasmussen, G., 1996. Vandmiljø i Limfjorden 1995. Limfjordsovervågningen (Ringkøbing amtskommune, Viborg amt og Nordjyllands amt).

Gyllencreutz, R., 2005. Late glacial and Holocene paleoceanography in the Skagerrak from high-resolution grain size records. Palaeogeography, Palaeoclimatology, Palaeoecology 222, 344–369.

Gyllencreutz, R., Kissel, C., 2006. Lateglacial and Holocene sediment sources and transport patterns in the Skagerrak interpreted from high-resolution magnetic properties and grain size data. Quaternary Science Reviews 25, 1247–1364.

Haake, F.W., 1962. Untersuchungen an der foraminiferen-fauna im Wattgebiet zwischen Langeoog und dem Festland. Meyniana 12, 25–64.

Heier-Nielsen, S., 1992. Foraminferanalyse, ^{14}C-dateringer og stabil isotop analyse i kerne 95, Limfjorden. Dansk Geologisk Forening, Årsskrift 1990-1991, 39–45.

Heier-Nielsen, S., Heinemeier, J., Nielsen, H.L., Rud, N., 1995. Recent reservoir ages for Danish fjords and marine waters. Radiocarbon, 37, 875-882.

Hilton, J., 1985. A conceptual framework for predicting the occurrence of sediment focusing and sediment redistribution in small lakes. Limnology and Oceanography 30, 1131-1143.

Hofmeister, R., Bolding, K., Burchard, H., 2006. Managing benthic ecosystems in relation to physical forcing and environmental constraints. MaBenE Deliverable D1.1. Report about Limfjord model setup and results, pp. 19.

Iversen, J., 1941. Landnam i Danmarks Stenalder. Danmarks Geologiske Undersøgelse II 66, 68 pp.

Jeffrey, S., Mantoura, R., Wright, S., 1997. Phytoplankton pigments in oceanography: guidelines to modern methods. UNESCO publishing, Paris.

Jensen, J.P., Pedersen, A.R., Jeppesen, E., Søndergaard, M., 2006. An empirical model describing the seasonal dynamics of phosphorus in 16 shallow eutrophic lakes after external loading reduction. Limnology and Oceanography 51, 791–800.

Jiang, H., Björck, S., Knudsen, K.L., 1997. A palaeoclimatic and palaeoceanographic record of the last 11 000 ^{14}C years from the Skagerrak-Kattegat, northeastern Atlantic margin. The Holocene 7, 301–310.

Jones, V.J., Juggins, S., 1995. The construction of a diatom-based chlorophyll a transfer function and its application at three lakes in Signy Island (maritime Antarctic) subject to differing degrees of nutrient enrichment. Freshwater Biology 34, 433–445.

Juggins, S. (1991-2009) C2 data analysis. Newcastle University, Newcastle. http://www.staff.ncl.ac.uk/staff/stephen.juggins/software/C2Home.htm.

926 Juggins, S., 2001. The European diatom database user guide: Version 1.0. University of
927 Newcastle, Newcastle upon Tyne. 72pp.
928 Kabel, K., Moros, M., Porsche, C., Neumann, T., Adolphi, F., Andersen, T.J., Siegel, H.,
929 Gerth, M., Leipe, T., Jansen, E., Sinninghe Damsté, J.S., 2012. Impact of climate
930 change on the Baltic Sea ecosystem over the past 1,000 years. Nature Climate Change
931 2, 871–874.
932 Knudsen, K.L., 1998. Foraminiferer i Kvartær stratigrafi: Laboratorie- og fremstillingsteknik
933 samt udvalgte eksempler. Geologisk Tidsskrift 3, 1–25.
934 Kristensen, P., Heier-Nielsen, S., Hylleberg, J., 1995. Late-Holocene salinity fluctuations in
935 Bjørnsholm Bay, Limfjorden, Denmark, as deduced from micro- and macrofossil
936 analysis. The Holocene 5, 312–322.
937 Leavitt, P.R., Vinebrooke, R.D., Donald, D.B., Smol, J.P., Schindler, D.W., 1997. Past
938 ultraviolet radiation environments in lakes derived from fossil pigments. Nature 388,
939 457–459.
940 Leth, J.O., 1996. Late Quaternary geological development of the Jutland Bank and the
941 initiation of the Jutland Current, NE North Sea. Norges Geologiske Undersøkelse
942 Bulletin 430, 25–34.
943 Lewis, J.P., 2011. Holocene environmental change in coastal Denmark: interactions between
944 land, sea and society. Ph.D. Thesis, Loughborough University, Loughborough, UK.
945 Available from the Loughborough University Institutional Repository at:
946 http://hdl.handle.net/2134/8717
947 Lutze, G.F., 1965. Zur foraminiferenfauna der Ostsee. Meyniana 15, 75–142.
948 Lutze, G.F., 1974. Foraminiferen der Kieler Bucht (Westliche Ostsee): 1. 'Hausgartengebiet'
949 des Sonderforschungsbereiches 95 der Universität Kiel. Meyniana 26, 9–22.
950 Madsen, A.P., Müller, S., Neergaard, C., Petersen, C.G.J., Rostrup, E., Steenstrup, K.J.V.,
951 Winge, H., 1900. Affaldsdynger fra Stenalderen i Danmark. Undersøgte for
952 Nationalmuseet C.A. Reitzel, Copenhagen
953 Mannino, A., Harvey, H.R. 2000. Biochemical composition of particles and dissolved organic
954 matter along an estuarine gradient: sources and implications for DOM reactivity.
955 Limnology & Oceanography 45, 775–788.
956 Martin-Puertas, C., Matthes, K., Brauer, A., Muscheler, R., Hansen, F., Petrick, C., Aldahan,
957 A., Possnert, G., van Geel, B., 2012. Regional atmospheric circulation shifts induced
958 by a grand solar minimum. Nature Geoscience, DOI: 10.1038/NGEO1460.
959 Mayewski, P.A., Meeker, L.D., Twickler, M.S., Whitlow, S.I., Yang, Q., Lyons, W.B.,
960 Prentice, M., 1997. Major features and forcing of high-latitude Northern Hemisphere
961 atmospheric circulation using a 110,000- year-long glaciochemical series. Journal of
962 Geophysical Research 102, 26345–26366.
963 McGowan, S., 2007. Pigments in sediments of aquatic environments. In: Elias, S.A. (Ed.)
964 Encyclopedia of Quaternary Science, Elsevier, Amsterdam, pp. 2062–2074.
965 Mertens, K.N., Dale, B., Ellegaard, M., Jansson, I.-M., Godhe, A., Kremp, A., Louwye, S.,
966 2011. Process length variation in cysts of the dinoflagellate *Protoceratium*
967 *reticulatum*, from surface sediments of the Baltic–Kattegat–Skagerrak estuarine
968 system: a regional salinity proxy. Boreas 40, 242–255.
969 Mertz, E.L., 1924. Late and post-glacial height changes in Denmark (In Danish). Danish
970 Geological Survey (DGU) 2, række nr. 41, pp. 50.
971 Mikkelsen, P.H., 1994. Arkæozoologiske og arkæobotaniske undersøgelser af
972 bopladsmaterialet fra ældre jernalder. LAG 5, 73–114.
973 Moeslund, B., Løjtnant, B., Mathiesen, H., Mathiesen, L., Pedersen, A., Thyssen, N., Schou,
974 J.C., 1990. Danske vandplanter. Miljøministeriet, Miljøstyrelsen, Copenhagen.
975 Murray, J.W., 1991. Ecology and palaeoecology of benthic foraminifera. Longman, Harlow.

976 Murray, J.W., 2006. Ecology and applications of benthic foraminifera. Cambridge University
977 Press, Cambridge.
978 Neumann, T., Eilola, K., Gustafsson, B., Müller-Karulis, B., Kuznetsov, I., Markus Meier,
979 H.E., Savchuk, O.P., 2012. Extremes of temperature, oxygen and blooms in the Baltic
980 Sea in a changing climate. Ambio 41, 574–585.
981 Nielsen, N., 2008. Marine molluscs in Danish Stone Age middens: a case study on
982 Krabbesholm II. In: Antczak, A., Cipriani, R. (Eds.), Early human impact on
983 megamolluscs. BAR International Series, Volume 1865, Hadrian Books Ltd,
984 Banbury, Oxford, UK, pp. 157–167.
985 Odgaard, B., 1989. Cultural landscape development through 5500 years at Lake Skånsø,
986 North-western Jutland as reflected in a regional pollen diagram. Journal of Danish
987 Archaeology 8, 200–210.
988 Odgaard, B., 1994. The Holocene vegetation history of northern West Jutland. Opera
989 Botanica, 123, pp. 171.
990 Olsen, J., Rasmussen, P., Heinemeier, J., 2009. Holocene temporal and spatial variation in the
991 radiocarbon reservoir age of three Danish fjords. Boreas, 38, 458-470.
992 Olsen, J., Noe-Nygaard, N., Wolfe, B.B., 2010. Mid- to late-Holocene climate variability and
993 anthropogenic impacts: multi-proxy evidence from Lake Bliden, Denmark. Journal of
994 Paleolimnology 43, 323–343.
995 Pedersen, J.B.P., Svinth, S., Bartholdy, J., 2009. Holocene evolution of a drowned melt-water
996 valley in the Danish Wadden Sea. Quaternary Research 72, 68–79.
997 Petersen, K.-S., 1981. The Holocene marine transgression and its molluscan fauna in the
998 Skagerrak-Limfjord region, Denmark. Special Publications International Association
999 of Sedimentologists 5, 497–503.
1000 Petersen, K.-S., 2004. Late Quaternary environmental changes recorded in the Danish marine
1001 molluscan faunas. Geological Survey of Denmark and Greenland Bulletin, 3, pp. 268.
1002 Philippsen, B., Olsen, J., Lewis, J.P., Rasmussen, P., Ryves, D.B., Knudsen, K.L., in press.
1003 Mid- to late-Holocene reservoir age variability and isotope based
1004 palaeoenvironmental reconstruction in the Limfjord, Denmark. The Holocene. DOI:
1005 10.1177/0959683613479681.
1006 Poulsen, B., Holm, P., MacKenzie, B.R., 2007. A long-term (1667-1860) perspective on
1007 impacts of fishing and environmental variability for herring, eel. and whitefish in the
1008 Limfjord, Denmark. Fisheries Research 2-3, 181–195.
1009 Poulsen, K.L., 1978. Eisenzeitliche muschelhaufen in Dänemark. Offa 35, 64-85.
1010 Ramsey, C.B., 2008. Deposition models for chronological records. Quaternary Science
1011 Reviews 27, 42–60.
1012 Rasmussen, H., 1968. Limfjordsfiskeriet før 1825. Sædvane og centraldirigering. Folkelivs
1013 studier 2, Copenhagen, Denmark.
1014 Rasmussen, M., 1992. Fisker og bonde i ældre bronzealder. Limfjordsprojektet:
1015 Limfjordsfiskeri i fortid og nutid, Rapport no. 4, 97–106.
1016 Rasmussen, P., 2005. Mid- to late-Holocene land-use change and lake development at
1017 Dallund Sø, Denmark: vegetation and land-use history inferred from pollen data. The
1018 Holocene 15, 1116–1129.
1019 Reimer, P.J., Baillie, M.G.L., Bard, E., Bayliss, A., Beck, J.W., Blackwell, P.G., Ramsey,
1020 C.B., Buck, C.E., Burr, G.S., Edwards, R.L., Friedrich, M., Grootes, P.M.,
1021 Guilderson, T.P., Hajdas, I., Heaton, T.J., Hogg, A.G., Hughen, K.A., Kaiser, K.F.,
1022 Kromer, B., McCormac, F.G., Manning, S.W., Reimer, R.W., Richards, D.A.,
1023 Southon, J.R., Talamo, S., Turney, C.S.M., van der Plicht, J., Weyhenmeye, C.E.,
1024 2009. Intcal09 and Marine09 radiocarbon age calibration curves, 0-50,000 years cal.
1025 BP. Radiocarbon 51, 1111–1150.

Renberg, I., 1990. A procedure for preparing large sets of diatom slides from sediment cores. Journal of Paleolimnology 4, 87–90.
Reuss, N., Conley, D.J., Bianchi, T.S., 2005. Preservation conditions and the use of sediment pigments as a tool for recent ecological reconstruction in four Northern European estuaries. Marine Chemistry 95, 283–302.
Ringtved, J., 1992. Fiskeri i jernalderen (500 f.Kr.-1050 e.Kr.) - et overset erhvervsaspekt? Limfjordsprojektet: Limfjordsfiskeri i fortid og nutid, Rapport no. 4, 107–124.
Ringtved, J., 1998. Landbo og fjordbo – regionale betragtninger om Limfjordsområdet, Limfjordsprojektet: Variation og enhed omkring Limfjorden, Rapport no. 8, 39–83.
Rouvillois, A., 1970. Biocoenose et taphocoenose de foraminifères sur le plateau continental Atlantique au large de l'Ile d'Yeu. Revue de Micropaléontology 13, 188–204.
Rowley-Conwy, P., 1984. The laziness of the short-distance hunter: the origins of agriculture in western Denmark. Journal of Anthropological Archaeology 3, 300–324.
Ryves, D.B., Clarke, A.L., Appleby, P.G., Amsinck, S.L., Jeppesen, E., Landkildehus, F., Anderson, N.J., 2004. Reconstructing the salinity and environment of the Limfjord and Vejlerne Nature Reserve, Denmark, using a diatom model for brackish lakes and fjords. Canadian Journal of Fisheries and Aquatic Sciences, 61 1988–2006.
Ryves, D.B., Battarbee, R.W., Juggins, S., Fritz, S.C. Anderson, N.J., 2006. Physical and chemical predictors of diatom dissolution in freshwater and saline lake sediments in North America and West Greenland, Limnology & Oceanography 51, 1355-1368
Ryves, D.B., Battarbee, R.W., Fritz, S.C., 2009. The dilemma of disappearing diatoms: incorporating diatom dissolution data into palaeoenvironmental modelling and reconstruction. Quaternary Science Reviews 28, 120–136.
Schulting, R. 2010. Holocene environmental change and the Mesolithic-Neolithic transition in north-west Europe: revisiting two models. Environmental Archaeology 15, 160–172.
Scully, N.M., Lean, D.R.S., 1994. The attenuation of ultraviolet radiation in temperate lakes. Archiv für Hydrobiologie 43, 135–144.
Seppä, H., Bjune, A.E., Telford, R.J., Birks, H.J.B., Veski, S., 2009. Last nine-thousand years of temperature variability in Northern Europe. Climate of the Past 5, 523–535.
Sharp, Z., 2007. Principles of Stable Isotope Geochemistry. Pearson Prentice Hall, Upper Saddle River, New Jersey.
Smittenberg, R.H., Pancost, R.D., Hopmans, E.C., Paetzel, M., Sinninghe Damsté, J.S.S., 2004. A 400-year record of environmental change in an euxenic fjord as revealed by the sedimentary biomarker record. Palaeogeography, Palaeoclimatology, Palaeoecology 202, 331–351.
Snowball, I., Korhola, A., Briffa, K.R., Koç, N., 2004. Holocene climate dynamics in Fennoscandia and the North Atlantic. In: Battarbee, R.W., Gasse, F., Stickley, C.E. (Eds.) Past climate variability through Europe and Africa. Kluwer Academic Publishers, Dordrecht, Netherlands, pp. 364–397.
Sorgenfrei, T., 1958. Molluscan assemblages from the marine middle Miocene of South Jutland and their environment. Danmarks Geologiske Undersøgelse II 79, 356–503.
Telford, R.J., Birks, H.J.B., 2005. The secret assumption of transfer functions: problems with spatial autocorrelation in evaluating model performance. Quaternary Science Reviews, 24, 2173–2179.
ter Braak, C.J.F., Šmilauer, P., 2002. CANOCO reference manual and CanoDraw for Windows users' guide: Software for Canonical Community Ordination (version 4.5). Microcomputer Power, Ithaca, New York, USA.
Troels-Smith, J., 1955. Karakterisering af løse jordarter. Danmarks Geologiske Undersøgelse, Series IV/3 10, 1–73.

Wachnicka, A., Gaiser, E., Collins, L., Frankovich, T., & Boyer, J., 2010. Distribution of diatoms and development of diatom-based models for inferring salinity and nutrient concentrations in Florida Bay and adjacent coastal wetlands of south Florida (USA). Estuaries and Coasts 33, 1080–1098.

Walton, W.R., Sloan, B.J., 1990. The genus *Ammonia* Brünnich, 1772 its geographic distribution and morphologic variability. Journal of Foraminiferal Research 20, 128–156.

Windolf, J., Jeppesen, E., Jensen, J.P., Kristensen, P., 1996. Modelling of seasonal variation in nitrogen retention and in-lake concentration: a four-year mass balance study in 16 shallow Danish lakes. Biogeochemistry 33, 25–44.

Yonge, C.M., 1960. Oysters. Collins, London.

Yu, S.-Y., 2003. Centennial-scale cycles in middle Holocene sea level along the southeastern Swedish Baltic coast. GSA Bulletin 114, 1404–1409.

Yu, S.Y., Berglund, B.E., 2007. A dinoflagellate cyst record of Holocene climate and hydrological changes along the southeastern Swedish Baltic coast. Quaternary Research 67, 215–224.

Figure 1. A) Location map showing the position of the Limfjord and the study site Kilen. Dotted lines represent haloclines of modern surface salinity (in g L^{-1}) and black arrows represent major present day current patterns in the Skagerrak, Kattegat and eastern North Sea (after Gyllencreutz and Kissel, 2006). Abbreviations: NCC = Norwegian coastal current, NJC = North Jutland current, SJC = South Jutland current, AW = Atlantic water, BC = Baltic current, BW = Baltic water, CNSW = Central North Sea water, JB = approximate location of the Jutland Bank. B) Map of the Limfjord indicating the position of the study site and Mesolithic/Neolithic shell middens (red dots; after Andersen, 1992b). Dotted line indicates proposed shoreline during the late Mesolithic (after Andersen, 1992b). Abbreviations: JB = Jutland Bank, AC = Agger channel. C) Map of the Kilen sedimentary basin including major fluvial inputs, basic bathymetry and key catchment characteristics (after Jensen et al., 2006). Coring location is marked with a black star. The Kilerkanal (labelled) connects the Kilen basin with the Limfjord and is responsible for maintaining brackish salinity. Abbreviations: Br. = Bremdal, SB = Struer Bugt.

Figure 2. Oxcal (v 4.1) based age-depth model for the Kilen profile. Dotted lines refer to boundaries (i.e. depth levels) in the age model where the accumulation rate is allowed change substantially (based on $CaCO_3$ weight%; see Philippsen et al., in press).

Figure 3. Kilen lithology and sedimentary parameters, including overall sedimentary accumulation rate (cm/yr), water content/dry mass (expressed as a percentage of the total sediment wet weight), accumulation (mg cm yr^{-1}) of organic matter, calcium carbonate ($CaCO_3$), minerogenic matter, selected sedimentary pigments (pmol cm^{-2} yr^{-1}) and associated metrics (i.e. Pheophytin-*a*/chlorophyll *a* ratio and UV-R index). Ultraviolet index (UV-R index) after Leavitt et al., (1997): UV-C/(alloxanthin + diatoxanthin + lutein-zeaxanthin) x 100. *Plot displayed on independent scaling.

Figure 4. Kilen plant macrofossil and molluscan records (selected species), expressed as concentration (no. per 50 ml of sediment). Molluscs ordered via class (bivalvia or gastropoda) and minimum salinity tolerance (i.e. values in brackets in g L^{-1}) after Sorgenfrei (1958). *Plot displayed on independent scaling.

Figure 5. Kilen percentage diatom record (selected taxa). Numbers in brackets refer to the weighted averaged salinity optima in the Molten training set used for the quantitative reconstruction of salinity. Modern surface salinity range (grey shading) provided for the Struer Bugt area based on Burman and Schmitz, (2005) and Hofmeister et al., (2006).

Figure 6. Kilen diatom associated metrics including diatom concentration (per g dw; dry weight) and flux (no. per cm^{-2} yr^{-1}), Hills N_2 diversity index, diatom dissolution (**F** index: Ryves et al., 2009), pelagic: benthic: tychopelagic ratios diatom-inferred salinity (g L^{-1}) and goodness of fit between the fossil data and the DI-salinity model at each level (see text for details). P1-3 = Phases of decline in pelagic diatom abundance referred to in the text.

Figure 7. Kilen percentage foraminifera record (selected taxa) including foraminifera concentration (no. per 10 ml of sediment), foraminifera flux (no. cm^{-2} yr^{-1}) and $\delta^{18}O$ and $\delta^{13}C$ isotopes based on tests of the benthic foraminifer *Elphidium excavatum* f. *selseyensis*.

Figure 8. Comparison of the Kilen multiproxy data with regional hydrographic and climate proxies. A) Stratification indicators: high-salinity foraminifera = summed abundance of *Elphidium incertum, Elphidium magellanicum, Elphidium margaritaceum, Haynesina depressula, Stainforthia* sp. and *Bulimina marginata*. P1-3 = Pelagic declines (see text). B) Diatom-inferred salinity, with aeolian events "A2-A4" identified in Clemmensen et al., 2009 and water column state (inferred from this study). C) Ultraviolet radiation (UV-R) index. D) Sedimentary pigment accumulation: smoothed curves (0.1 span) for total (left axis), okenone and echinenone (right axis). E) Total mollusc concentration. F) Sortable silt (core MD99-2286) and estimated Holocene bottom current strength evolution in the Skagerrak (from Gyllencreutz and Kissel, 2006) and timing of the drowning of the Jutland Bank (JB; Leth, 1996). G) Pollen-inferred mean annual air temperature (^{o}C) at Lake Trehörningen, Sweden (Antonsson and Seppä, 2007). Grey shaded area covers the brackish period, when the Limfjord was isolated from the North Sea and Skagerrak. Cultural divisions after Fischer and Kristiansen (2002); KON = Kongemose, EN = Early Neolithic, MNA = Middle Neolithic A, MNB = Middle Neolithic B, LN = Late Neolithic, EBA = Early bronze Age, LBA = Late Bronze Age, PRIA = Pre Roman Iron Age, RIA = Roman Iron Age, GIA = Germanic Iron Age.

Table 1. Training set details, performance statistics of tested diatom salinity models and comparison with other diatom-based salinity models from coastal environments. *Transfer function model selected for final diatom-inferred salinity reconstruction at Kilen over the study period.

Table

Modern training set:		
No. of samples	210	
No. of species	309	
Salinity gradient	0 - 31 g L^{-1}	
Tested salinity models:	**r^2_{boot}**	**RMSEP (square root salinity g L^{-1})**
Modern analogue technique	0.91	0.38
Maximum likelihood	0.89	0.41
Weighted averaging (inverse)	0.89	0.40
Weighted averaging partial least squares_component 2*	0.91	0.37
Other coastal salinity transfer functions examples:	**r^2_{jack}**	**RMSEP (g L^{-1})**
Ryves et al., (2004)	0.87	0.246* (log salinity)
Wachnika et al., (2010)	0.95	0.33 (square root salinity)

*Figure
Click here to download high resolution image

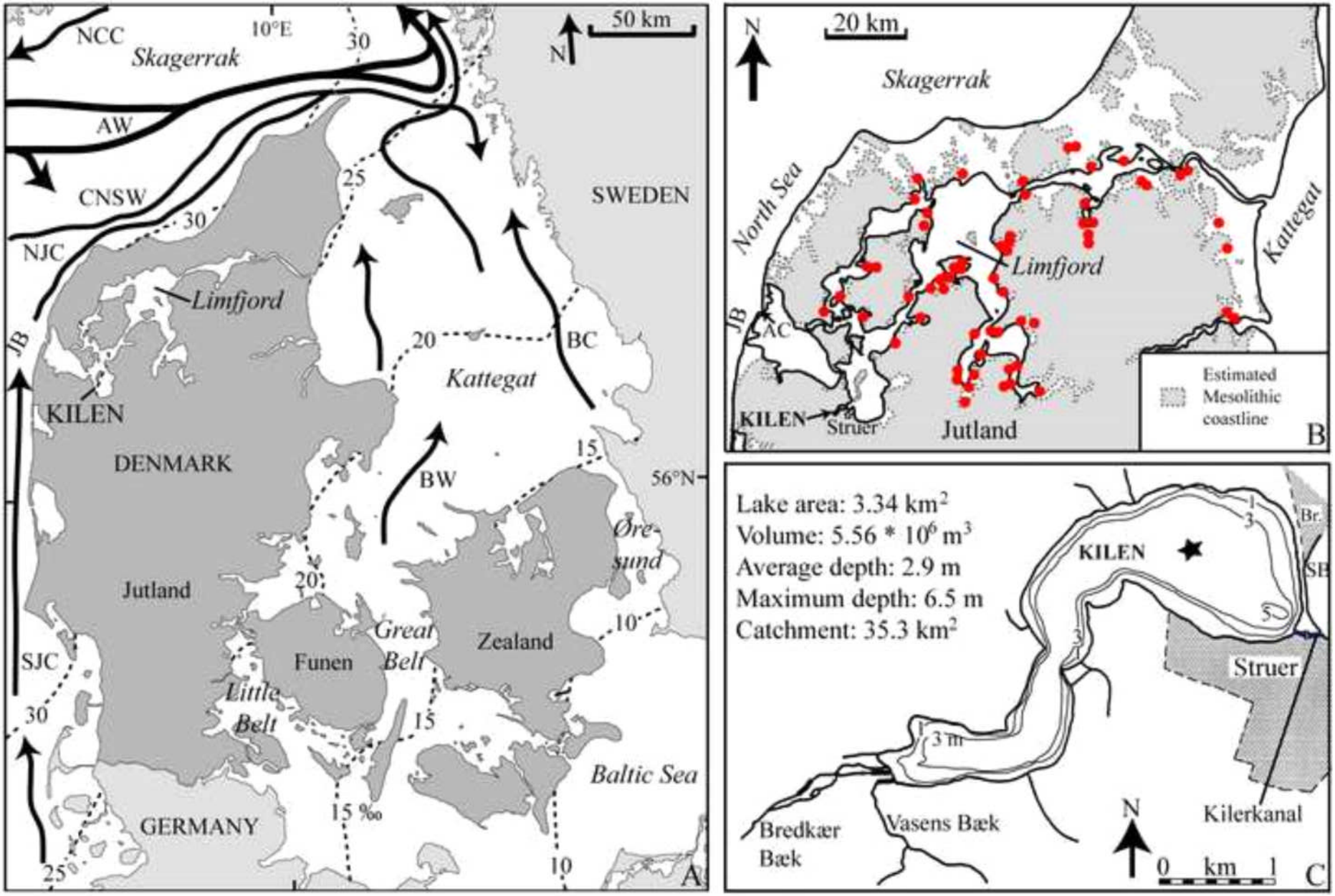

*Figure
Click here to download high resolution image

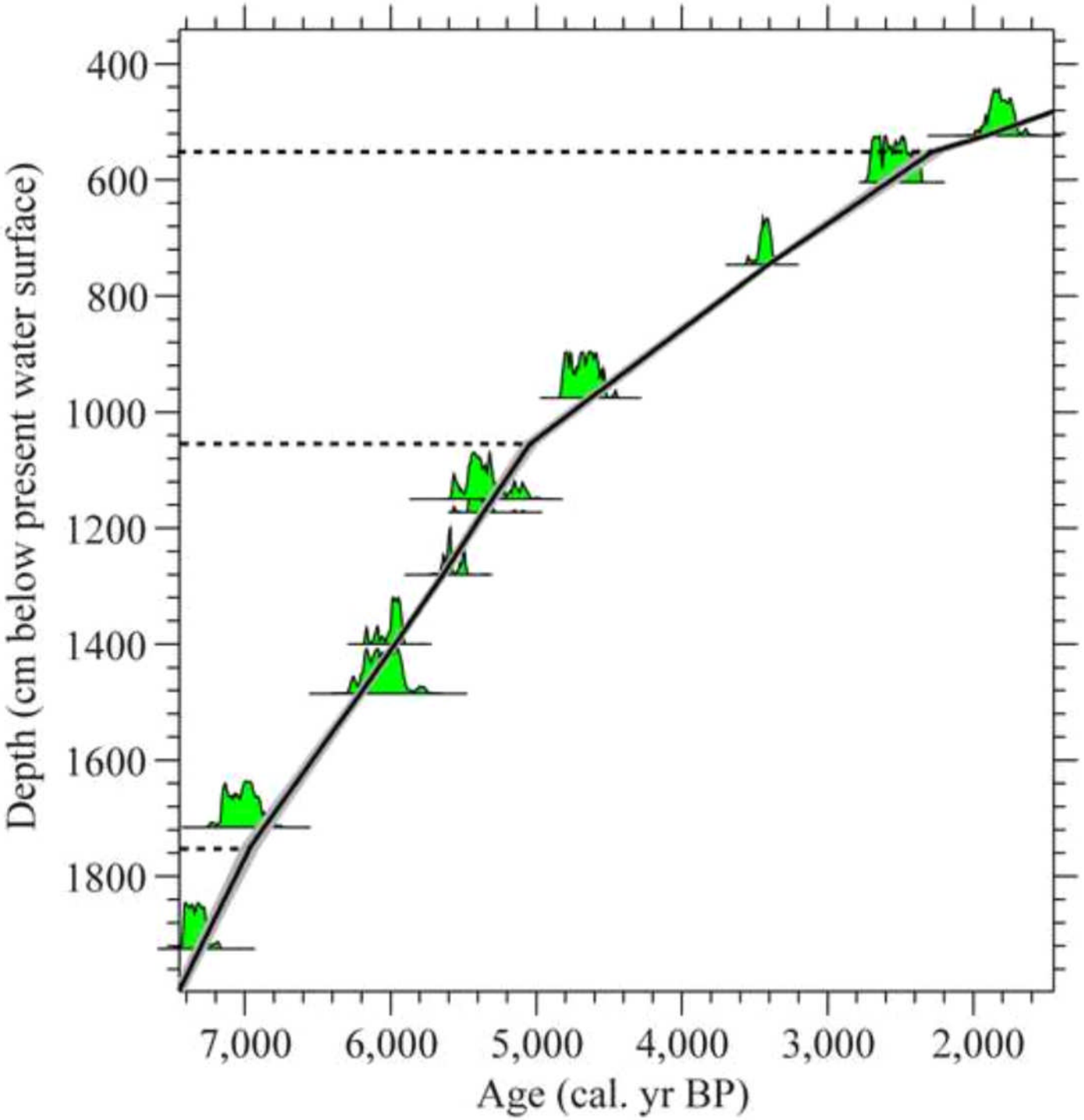

*Figure

Click here to download high resolution image

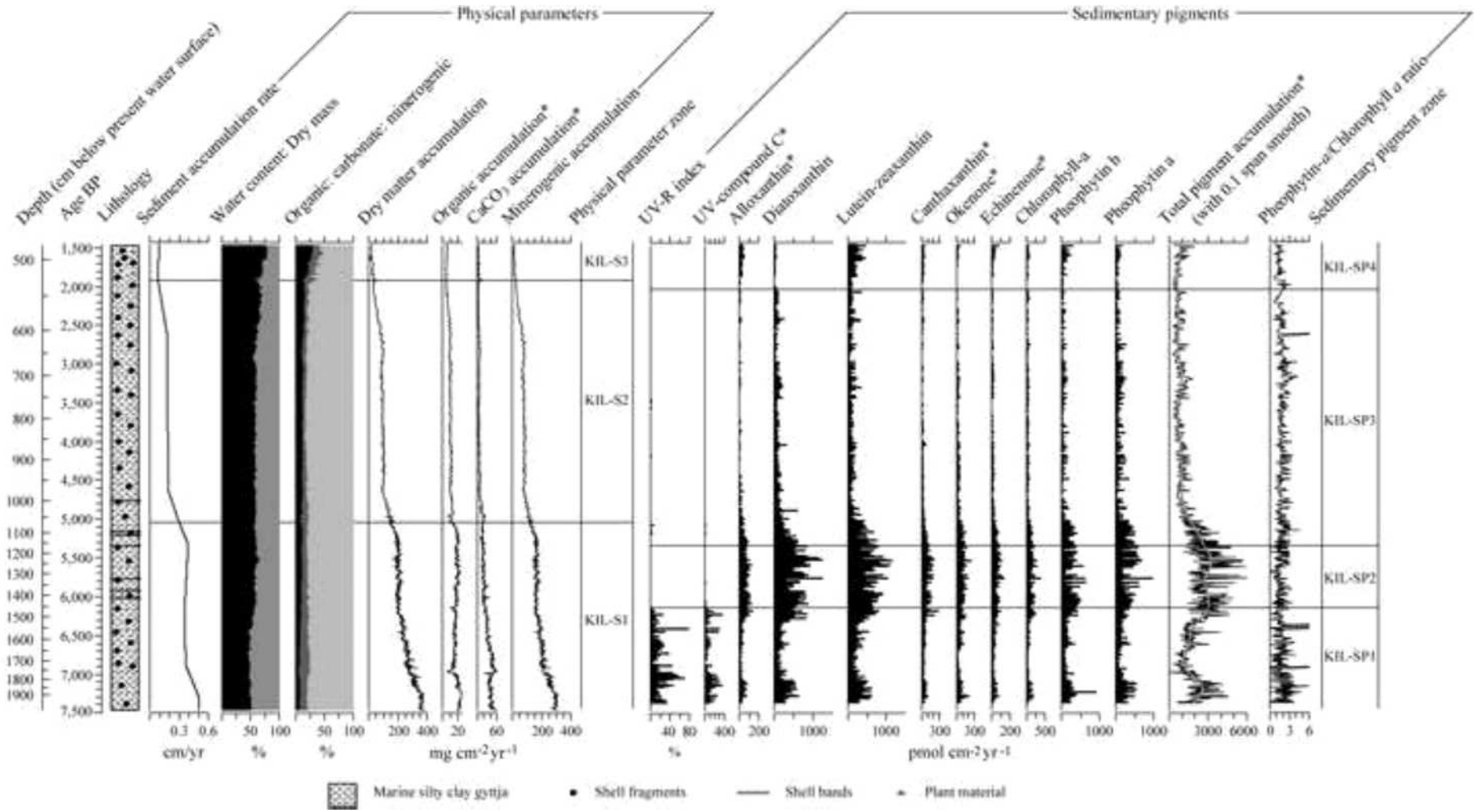

*Figure
Click here to download high resolution image

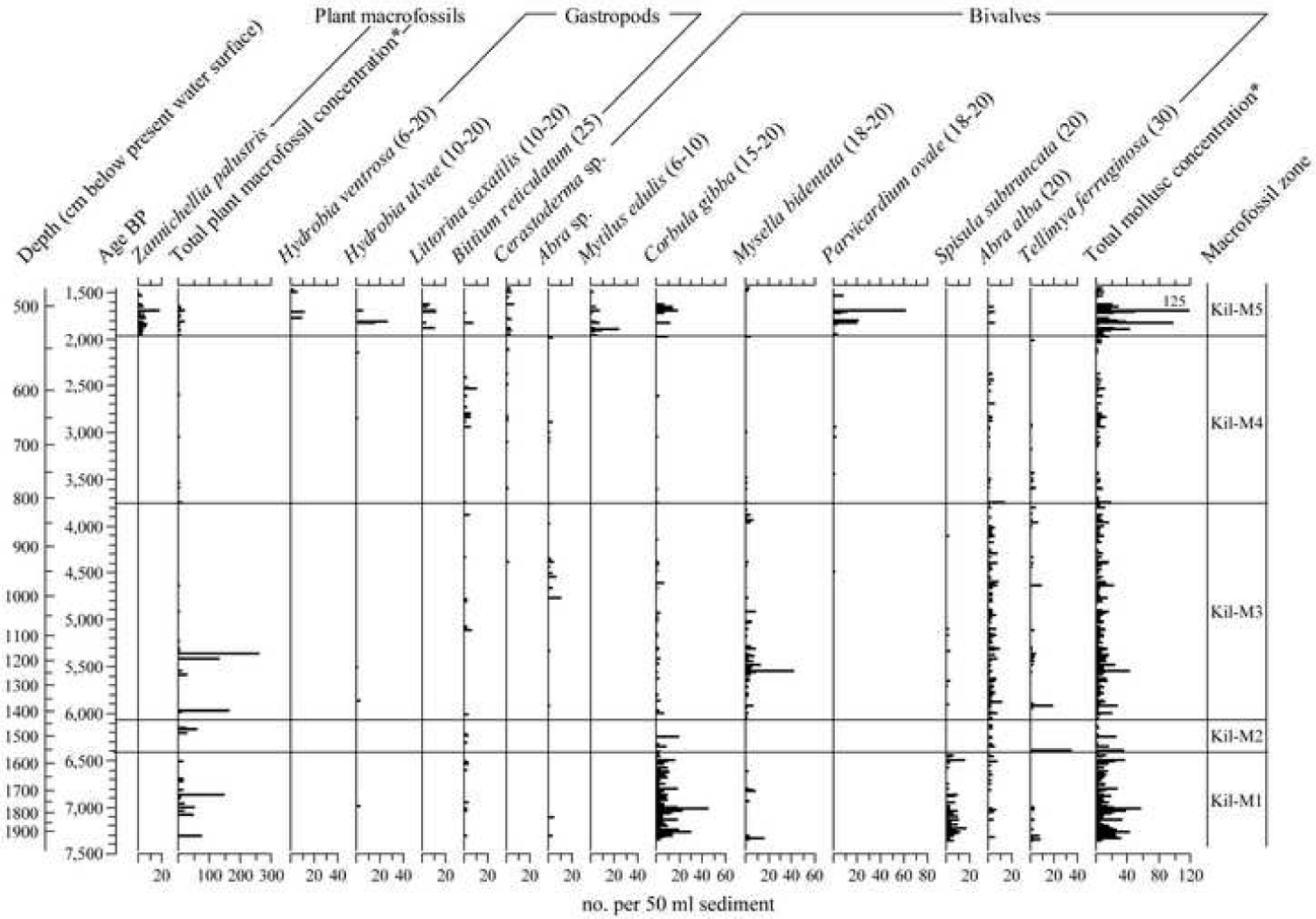

*Figure

Click here to download high resolution image

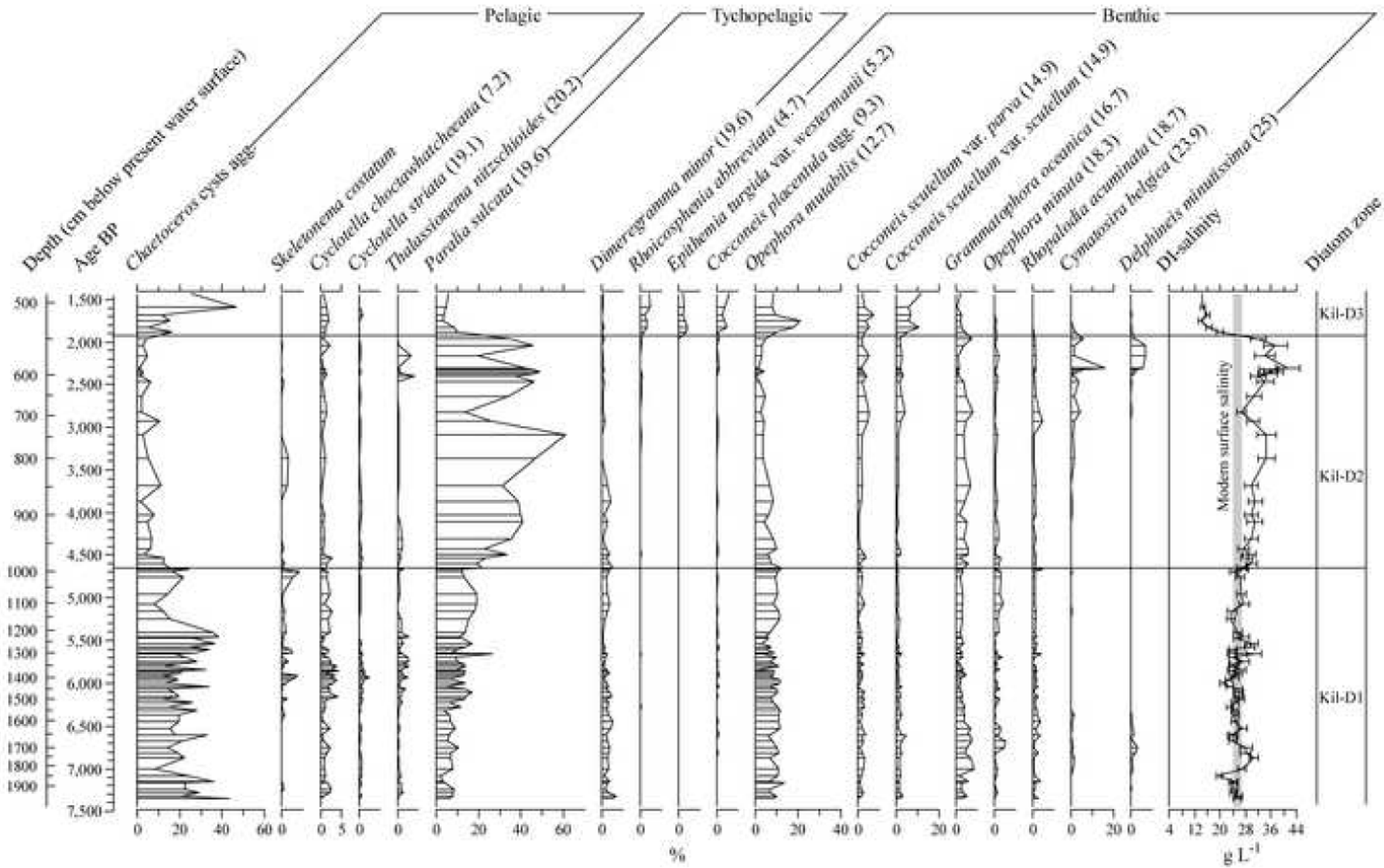

*Figure

Click here to download high resolution image

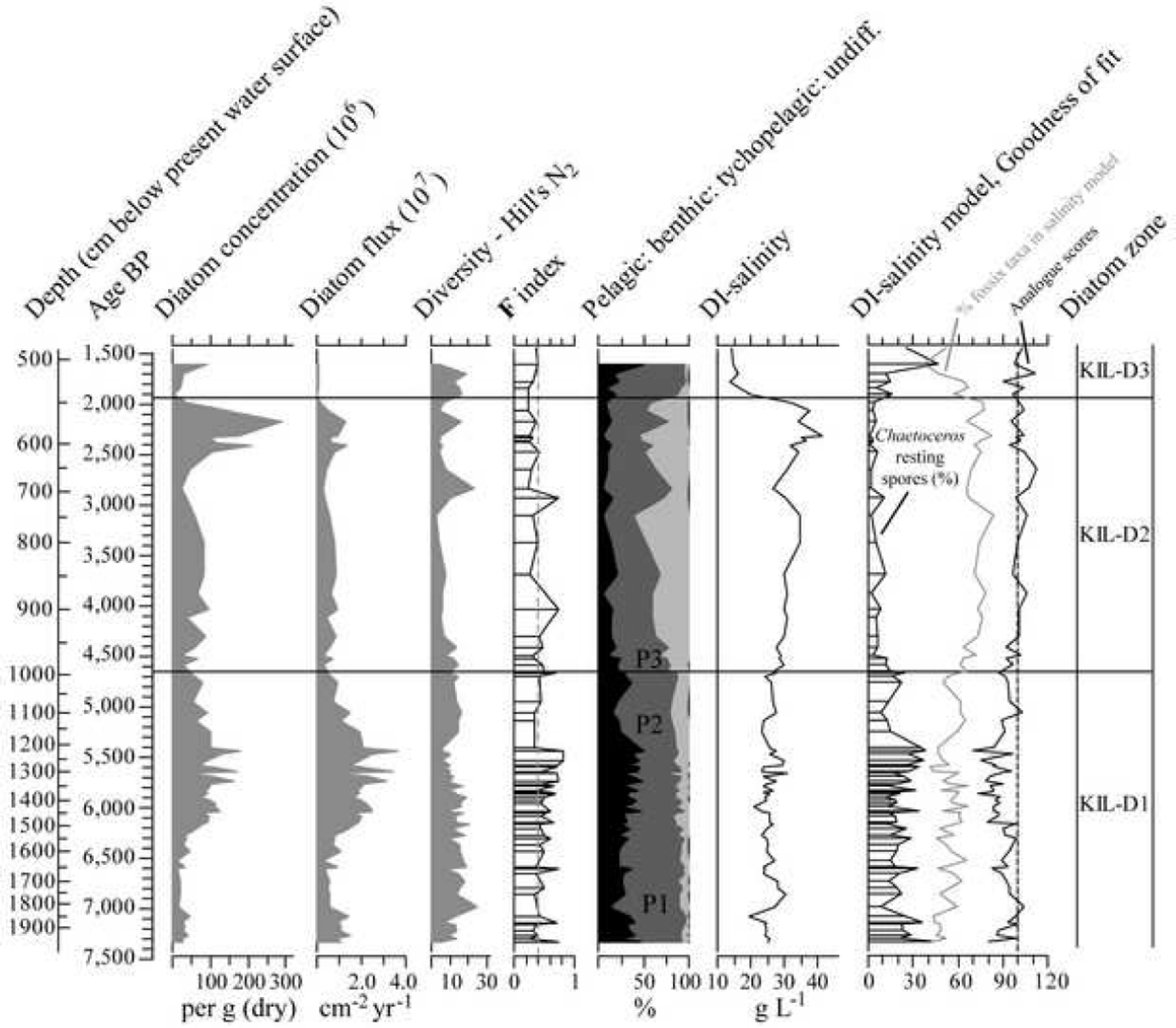

*Figure

Click here to download high resolution image

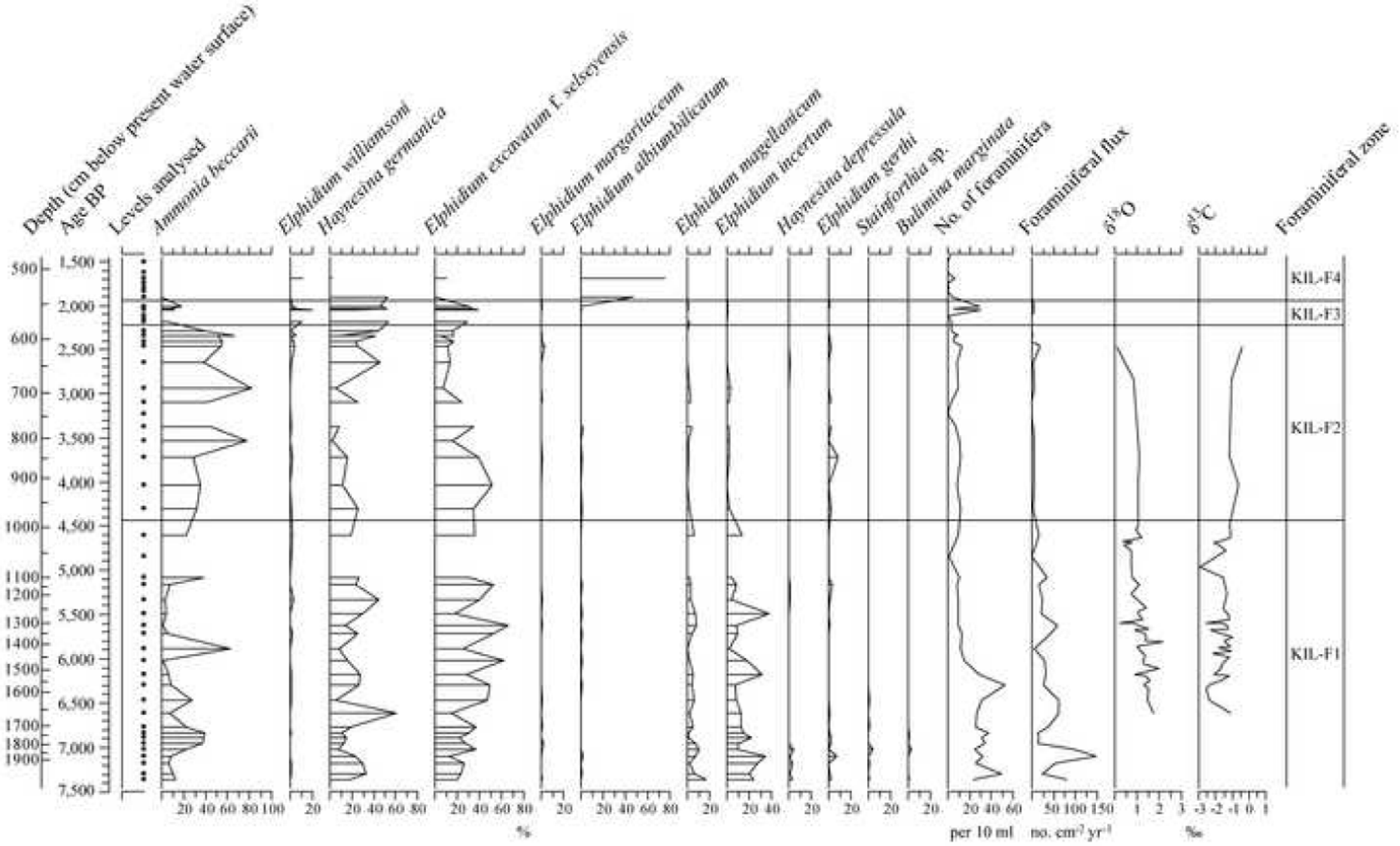

*Figure
Click here to download high resolution image